Explicit symplectic integrators of molecular dynamics algorithms for rigid-body molecules in the canonical, isobaric-isothermal, and related ensembles

Hisashi Okumura, Satoru G. Itoh, and Yuko Okamoto

Citation: J. Chem. Phys. **126**, 084103 (2007); doi: 10.1063/1.2434972
View online: https://doi.org/10.1063/1.2434972
View Table of Contents: http://aip.scitation.org/toc/jcp/126/8
Published by the American Institute of Physics

Explicit symplectic integrators of molecular dynamics algorithms for rigid-body molecules in the canonical, isobaric-isothermal, and related ensembles

Hisashi Okumura,[a] Satoru G. Itoh,[b] and Yuko Okamoto[c]
Department of Physics, School of Science, Nagoya University, Furo-cho, Chikusa-ku, Nagoya, Aichi 464-8602, Japan

(Received 12 October 2006; accepted 28 December 2006; published online 26 February 2007)

The authors propose explicit symplectic integrators of molecular dynamics (MD) algorithms for rigid-body molecules in the canonical and isobaric-isothermal ensembles. They also present a symplectic algorithm in the constant normal pressure and lateral surface area ensemble and that combined with the Parrinello-Rahman algorithm. Employing the symplectic integrators for MD algorithms, there is a conserved quantity which is close to Hamiltonian. Therefore, they can perform a MD simulation more stably than by conventional nonsymplectic algorithms. They applied this algorithm to a TIP3P pure water system at 300 K and compared the time evolution of the Hamiltonian with those by the nonsymplectic algorithms. They found that the Hamiltonian was conserved well by the symplectic algorithm even for a time step of 4 fs. This time step is longer than typical values of 0.5–2 fs which are used by the conventional nonsymplectic algorithms.
 [DOI: 10.1063/1.2434972]

I. INTRODUCTION

There are two models for molecules in molecular dynamics (MD) simulations. One model is a rigid-body model and the other is a flexible model. Relative coordinates in a molecule are fixed in the rigid-body model, while they vary in the flexible model. Because degrees of freedom in the rigid-body model are fewer than in the flexible model, the simulational cost is less expensive. Several MD techniques have thus been proposed for rigid-body molecules.

One possibility for the rigid-body modeling is to constrain a bond length and a bond angle among atoms in the molecules such as in the SHAKE algorithm.[1] Although it is easy to write a computer program for this constraint algorithm, it requires iteration procedures to fulfill the constraint. It means that one has to perform implicit time development.

Another algorithm is a quaternion scheme which gives explicit time development. One integrator to carry out a quaternion MD simulation is Gear's predictor-corrector algorithm.[2] However, this algorithm is not a symplectic integrator[3] nor time reversible. It hardly reflects characteristics of Hamiltonian dynamics. Another algorithm for the quaternion MD was proposed by Matubayasi and Nakahara.[4] Although this algorithm is not a symplectic integrator, it conserves volume in phase space and is time reversible. Miller *et al.* recently proposed a symplectic quaternion algorithm.[5] This algorithm also conserves volume in phase space and is time reversible. However, this symplectic quaternion algorithm has been proposed only in the microcanonical ensemble. There is no symplectic quaternion algorithm in the canonical ensemble and in the isobaric-isothermal ensemble.

A representative MD algorithm to obtain the canonical ensemble is the Nosé thermostat.[6,7] Because the original Nosé Hamiltonian gives dynamics in virtual time, a symplectic canonical MD simulation can be carried out in virtual time. However, a symplectic MD simulation cannot be realized in real time. Nonsymplectic integrators such as Gear's predictor-corrector algorithm are often employed for real-time development for the Nosé thermostat. Hoover improved the Nosé thermostat to propose the Nosé-Hoover thermostat.[8] Because the Nosé-Hoover thermostat is not based on a Hamiltonian, there is no symplectic algorithm[9] for the Nosé-Hoover thermostat. However, there exists an explicit time reversible integrator, although it does not conserve the volume in the phase space. This integrator was proposed by Martyna *et al.*[10] Bond *et al.* then proposed a symplectic constant temperature algorithm in real time, which is referred to as the Nosé-Poincaré thermostat.[11] However, the original symplectic algorithm for the Nosé-Poincaré thermostat is an implicit integrator. Iterations are necessary for the thermostat. Nosé improved the original algorithm and proposed an explicit symplectic integrator for the Nosé-Poincaré thermostat.[12] Although this formalism may not be widely known, we found it very powerful and useful as was shown in Refs. 13–15 and will be demonstrated below.

An explicit MD algorithm closest to a symplectic algorithm for rigid-body molecules in the canonical ensemble proposed so far is a combined algorithm[16] of the symplectic quaternion algorithm by Miller *et al.*[5] and time reversible algorithm for the Nosé-Hoover thermostat.[10] Because the Nosé-Hoover thermostat is a nonsymplectic algorithm, the whole algorithm is also nonsymplectic. Employing a symplectic MD algorithm, there is a conserved quantity which is

[a]Electronic mail: hokumura@tb.phys.nagoya-u.ac.jp
[b]Electronic mail: itoh@tb.phys.nagoya-u.ac.jp
[c]Electronic mail: okamoto@phys.nagoya-u.ac.jp

close to Hamiltonian and the long-time deviation of the Hamiltonian is suppressed. Symplectic MD algorithms are thus getting popular recently.

In this article, we propose an explicit symplectic MD algorithm for rigid-body molecules in the canonical ensemble. Our strategy is to combine the quaternion algorithm by Miller *et al.*[5] with the explicit symplectic algorithm for the Nosé-Poincaré thermostat by Nosé.[12] We further combine our algorithm with the Andersen barostat[17] to present an explicit symplectic MD algorithm for rigid-body molecules in the isobaric-isothermal ensemble. An explicit symplectic MD algorithm for spherical atoms in the isobaric-isothermal ensemble has been presented in Refs. 13 and 14. The isobaric-isothermal algorithm in this article is an extension of the algorithm for spherical atoms to that for rigid-body molecules. We also present a symplectic integrator in the constant normal pressure and lateral surface area ensemble and a symplectic integrator combined with the Parrinello-Rahman algorithm.

In Sec. II we first give brief reviews of the Nosé-Poincaré thermostat and the rigid-body MD algorithm. We then explain the symplectic MD algorithms for rigid-body molecules in the canonical, isobaric-isothermal, and related ensembles. In Sec. III we compare our symplectic MD algorithm with nonsymplectic MD algorithms in the canonical ensemble. We apply our symplectic MD algorithm to a rigid-body water model and make numerical comparisons with the nonsymplectic MD algorithms. Section IV is devoted to conclusions.

II. METHODS

A. Nosé-Poincaré thermostat

The Nosé-Poincaré Hamiltonian H_{NP} for N spherical atoms at temperature T_0 is given by[11,12]

$$H_{\mathrm{NP}} = s\left[\sum_{i=1}^{N}\frac{\boldsymbol{p}_i'^2}{2m_i s^2} + E(\boldsymbol{r}^{\{N\}}) + \frac{P_s^2}{2Q} + gk_BT_0\log s - H_0\right]$$
$$= s[H_{\mathrm{N}}(\boldsymbol{r}^{\{N\}},\boldsymbol{p}'^{\{N\}},s,P_s) - H_0], \tag{1}$$

where $\boldsymbol{p}_i'$ and P_s are the conjugate momenta for the coordinate $\boldsymbol{r}_i$ of particle i and Nosé's additional degree of freedom s, respectively, and k_B the is the Boltzmann constant. We have introduced a simplified notation by the superscript $\{N\}$ for the set of coordinate and momentum vectors: $\boldsymbol{r}^{\{N\}} \equiv (\boldsymbol{r}_1,\boldsymbol{r}_2,\ldots,\boldsymbol{r}_N)^T$ and $\boldsymbol{p}'^{\{N\}} \equiv (\boldsymbol{p}_1',\boldsymbol{p}_2',\ldots,\boldsymbol{p}_N')^T$, where the superscript T stands for transpose. The real momentum $\boldsymbol{p}_i$ and the virtual momentum $\boldsymbol{p}_i'$ are related by

$$\boldsymbol{p}_i = \frac{\boldsymbol{p}_i'}{s}. \tag{2}$$

E is the potential energy. The constant m_i is the mass of particle i and Q is the artificial "mass" associated with s. The constant g corresponds to the number of degrees of freedom. In the case of a spherical atomic system, g equals $3N$ (g equals $6N$ in the case of a rigid-body molecular system). The Hamiltonian H_{N} is the original Nosé Hamiltonian and H_0 is the initial value of H_{N}.

The equations of motion for the Nosé-Poincaré thermostat are given by

$$\dot{\boldsymbol{r}}_i = \frac{\boldsymbol{p}_i}{m_i}, \tag{3}$$

$$\dot{\boldsymbol{p}}_i = \boldsymbol{F}_i - \frac{\dot{s}}{s}\boldsymbol{p}_i, \tag{4}$$

$$\dot{s} = s\frac{P_s}{Q}, \tag{5}$$

$$\dot{P}_s = \sum_{i=1}^{N}\frac{\boldsymbol{p}_i^2}{m_i} - gk_BT_0, \tag{6}$$

where the dot above each variable stands for the time derivative and the relation of

$$H_{\mathrm{N}} - H_0 = 0 \tag{7}$$

is used because H_{N} is conserved. Equations (3)–(6) are the same as those for the Nosé thermostat in the real time.

B. Molecular dynamics algorithm for rigid-body molecules in the microcanonical ensemble

Hamiltonian for rigid-body molecules H_{RB} are given by[5,18]

$$H_{\mathrm{RB}} = \sum_{i=1}^{N}\frac{1}{8}\boldsymbol{\pi}_i^T\overleftrightarrow{\boldsymbol{S}}(\boldsymbol{q}_i)\overleftrightarrow{\boldsymbol{D}}_i\overleftrightarrow{\boldsymbol{S}}^T(\boldsymbol{q}_i)\boldsymbol{\pi}_i + E(\boldsymbol{q}^{\{N\}}), \tag{8}$$

where $\boldsymbol{q}_i$ is a quaternion of molecule i, which indicates the orientation of the rigid-body molecule. Here, the quaternion $\boldsymbol{q}=(q_0,q_1,q_2,q_3)^T$ is related to the Euler angle (ϕ,θ,ψ) as follows:

$$q_0 = \cos\left(\frac{\theta}{2}\right)\cos\left(\frac{\phi+\psi}{2}\right), \tag{9}$$

$$q_1 = \sin\left(\frac{\theta}{2}\right)\cos\left(\frac{\phi-\psi}{2}\right), \tag{10}$$

$$q_2 = \sin\left(\frac{\theta}{2}\right)\sin\left(\frac{\phi-\psi}{2}\right), \tag{11}$$

$$q_3 = \cos\left(\frac{\theta}{2}\right)\sin\left(\frac{\phi+\psi}{2}\right). \tag{12}$$

The elements of the matrix $\boldsymbol{S}(\boldsymbol{q})$ are given by

$$\overleftrightarrow{\boldsymbol{S}}(\boldsymbol{q}) = \begin{pmatrix} q_0 & -q_1 & -q_2 & -q_3 \\ q_1 & q_0 & -q_3 & q_2 \\ q_2 & q_3 & q_0 & -q_1 \\ q_3 & -q_2 & q_1 & q_0 \end{pmatrix}. \tag{13}$$

The variable $\boldsymbol{\pi}_i$ is the conjugate momentum for $\boldsymbol{q}_i$. The matrix $\overleftrightarrow{\boldsymbol{D}}$ is a 4×4 matrix consisting of the inverse of the principal moments of inertia I_1, I_2, and I_3 of molecule i,

$$\overleftrightarrow{D} = \begin{pmatrix} I_0^{-1} & 0 & 0 & 0 \\ 0 & I_1^{-1} & 0 & 0 \\ 0 & 0 & I_2^{-1} & 0 \\ 0 & 0 & 0 & I_3^{-1} \end{pmatrix}, \tag{14}$$

where I_0 is an artificial constant. Note that the correct equations of motion for rigid-body molecules are obtained in the limit of $I_0 \to \infty$. In order to write the equations of motion more elegantly, we may introduce the angular velocity

$$\boldsymbol{\omega} = (\omega_1, \omega_2, \omega_3)^T, \tag{15}$$

and the four-dimensional angular velocity

$$\boldsymbol{\omega}^{(4)} = (0, \omega_1, \omega_2, \omega_3)^T, \tag{16}$$

where ω_1, ω_2, and ω_3 are the angular velocities along each of the corresponding principal axes. In the limit of $I_0 \to \infty$, the four-dimensional angular velocity $\boldsymbol{\omega}_i^{(4)}$ is related to $\boldsymbol{\pi}_i$ by

$$\boldsymbol{\omega}_i^{(4)} = \frac{1}{2}\overleftrightarrow{D}_i \overleftrightarrow{S}^T(\boldsymbol{q}_i)\boldsymbol{\pi}_i. \tag{17}$$

In this limit the equations of motion for rigid-body molecules are obtained as follows:

$$\dot{\boldsymbol{q}}_i = \frac{1}{2}\overleftrightarrow{S}(\boldsymbol{q}_i)\boldsymbol{\omega}_i^{(4)}, \tag{18}$$

$$\overleftrightarrow{I}_i \dot{\boldsymbol{\omega}}_i = \boldsymbol{N}_i - \boldsymbol{\omega}_i \times (\overleftrightarrow{I}_i \boldsymbol{\omega}_i). \tag{19}$$

Equation (19) is called the Euler equation of motion. Here, $\boldsymbol{I}$ is the 3×3 diagonal matrix whose diagonal elements are I_1, I_2, and I_3. The vector $\boldsymbol{N}_i$ is the torque acting on molecule i, which is calculated by

$$\boldsymbol{N}_i = \sum_{\alpha \in i} \boldsymbol{r}_\alpha \times \boldsymbol{F}_\alpha, \tag{20}$$

where $\boldsymbol{F}_\alpha$ and $\boldsymbol{r}_\alpha$ are the coordinate and force of atom α, respectively, in a rigid-body-fixed coordinate system for molecule i. The torque $\boldsymbol{N}_i$ is related to the potential energy E by

$$-\frac{\partial E}{\partial \boldsymbol{q}_i} = 2\overleftrightarrow{S}(\boldsymbol{q}_i)\boldsymbol{N}_i^{(4)}, \tag{21}$$

where

$$\boldsymbol{N}_i^{(4)} = \left(\sum_{\alpha \in i} \boldsymbol{r}_\alpha \cdot \boldsymbol{F}_\alpha, \sum_{\alpha \in i} \boldsymbol{r}_\alpha \times \boldsymbol{F}_\alpha\right). \tag{22}$$

C. Symplectic molecular dynamics algorithm for rigid-body molecules combined with the Nosé-Poincaré thermostat

We here present the explicit symplectic MD algorithm for rigid-body molecules in the canonical ensemble. We combine the Nosé-Poincaré Hamiltonian in Eq. (1) (Refs. 11 and 12) and the Hamiltonian for rigid-body molecules in Eq. (8).[5,18] The Nosé-Poincaré Hamiltonian for rigid-body molecules is given by

$$H_{\text{NP-RB}} = s\left[\sum_{i=1}^{N} \frac{\boldsymbol{p}_i'^2}{2m_i s^2} + \sum_{i=1}^{N} \frac{1}{8s^2}\boldsymbol{\pi}_i'^T \overleftrightarrow{S}(\boldsymbol{q}_i)\overleftrightarrow{D}_i \overleftrightarrow{S}^T(\boldsymbol{q}_i)\boldsymbol{\pi}_i' + E(\boldsymbol{r}^{\{N\}}, \boldsymbol{q}^{\{N\}}) + \frac{P_s^2}{2Q} + gk_BT_0 \log s - H_0\right], \tag{23}$$

where $\boldsymbol{r}^{\{N\}} = (\boldsymbol{r}_1, \boldsymbol{r}_2, \ldots, \boldsymbol{r}_N)^T$ stands for the set of the coordinates of the center of mass for the rigid-body molecules. The vector $\boldsymbol{\pi}_i'$ is the conjugate momentum for quaternion $\boldsymbol{q}_i$. The real momentum $\boldsymbol{\pi}_i$ of the quaternion is related to the virtual momentum $\boldsymbol{\pi}_i'$ by

$$\boldsymbol{\pi}_i = \frac{\boldsymbol{\pi}_i'}{s}. \tag{24}$$

The equations of motion are given from the Hamiltonian in Eq. (23) by

$$\dot{\boldsymbol{r}}_i = \frac{\boldsymbol{p}_i}{m_i}, \tag{25}$$

$$\dot{\boldsymbol{p}}_i = \boldsymbol{F}_i - \frac{\dot{s}}{s}\boldsymbol{p}_i, \tag{26}$$

$$\dot{\boldsymbol{q}}_i = \frac{1}{2}\overleftrightarrow{S}(\boldsymbol{q}_i)\boldsymbol{\omega}_i^{(4)}, \tag{27}$$

$$\overleftrightarrow{I}_i \dot{\boldsymbol{\omega}}_i = \boldsymbol{N}_i - \boldsymbol{\omega}_i \times (\overleftrightarrow{I}_i \boldsymbol{\omega}_i) - \frac{\dot{s}}{s}\overleftrightarrow{I}_i \boldsymbol{\omega}_i, \tag{28}$$

$$\dot{s} = s\frac{P_s}{Q}, \tag{29}$$

$$\dot{P}_s = \sum_{i=1}^{N} \frac{\boldsymbol{p}_i^2}{m_i} + \sum_{i=1}^{N} \boldsymbol{\omega}_i^T \overleftrightarrow{I}_i \boldsymbol{\omega}_i - gk_BT_0. \tag{30}$$

The time development of a physical quantity $Z(\boldsymbol{\Gamma})$ in the phase space $\boldsymbol{\Gamma} \equiv (\boldsymbol{r}^{\{N\}}, \boldsymbol{p}'^{\{N\}}, \boldsymbol{q}^{\{N\}}, \boldsymbol{\pi}'^{\{N\}}, s, P_s)^T$ is written by

$$\frac{dZ}{dt} = \dot{\boldsymbol{\Gamma}} \cdot \frac{\partial Z}{\partial \boldsymbol{\Gamma}}. \tag{31}$$

The formal solution of the time development of Z from time t to $t + \Delta t$ is given by

$$Z(t + \Delta t) = \mathrm{e}^{D\Delta t} Z(t), \tag{32}$$

where $\mathrm{e}^{D\Delta t}$ is called a time propagator. The operator D is defined by

$$D \equiv \dot{\boldsymbol{\Gamma}} \cdot \frac{\partial}{\partial \boldsymbol{\Gamma}}. \tag{33}$$

In the symplectic algorithm, the Hamiltonian in Eq. (23) is separated into six terms here as follows:

$$H_{\text{NP-RB}} = H_{\text{NP-RB0}} + H_{\text{NP-RB1}} + H_{\text{NP-RB2}} + H_{\text{NP-RB3}} + H_{\text{NP-RB4}} + H_{\text{NP-RB5}}, \tag{34}$$

$$H_{\text{NP-RB0}} = s\sum_{i=1}^{N} \frac{1}{8I_0 s^2}(\boldsymbol{\pi}_i'^T \overleftrightarrow{\mathcal{P}}_0 \boldsymbol{q}_i)^2, \tag{35}$$

$$H_{\text{NP-RB1}} = s\left[\sum_{i=1}^{N}\frac{\boldsymbol{p}_i'^2}{2m_i s^2} + \sum_{i=1}^{N}\frac{1}{8I_1 s^2}(\boldsymbol{\pi}_i'^T\overleftrightarrow{\boldsymbol{\mathcal{P}}}_1\boldsymbol{q}_i)^2 + gk_BT_0\log s - H_0\right], \tag{36}$$

$$H_{\text{NP-RB2}} = s\sum_{i=1}^{N}\frac{1}{8I_2 s^2}(\boldsymbol{\pi}_i'^T\overleftrightarrow{\boldsymbol{\mathcal{P}}}_2\boldsymbol{q}_i)^2, \tag{37}$$

$$H_{\text{NP-RB3}} = s\sum_{i=1}^{N}\frac{1}{8I_3 s^2}(\boldsymbol{\pi}_i'^T\overleftrightarrow{\boldsymbol{\mathcal{P}}}_3\boldsymbol{q}_i)^2, \tag{38}$$

$$H_{\text{NP-RB4}} = sE(\boldsymbol{r}^{\{N\}},\boldsymbol{q}^{\{N\}}), \tag{39}$$

$$H_{\text{NP-RB5}} = s\frac{P_s^2}{2Q}, \tag{40}$$

where

$$\overleftrightarrow{\boldsymbol{\mathcal{P}}}_0\boldsymbol{q} = (q_0,q_1,q_2,q_3)^T, \tag{41}$$

$$\overleftrightarrow{\boldsymbol{\mathcal{P}}}_1\boldsymbol{q} = (-q_1,q_0,q_3,-q_2)^T, \tag{42}$$

$$\overleftrightarrow{\boldsymbol{\mathcal{P}}}_2\boldsymbol{q} = (-q_2,-q_3,q_0,q_1)^T, \tag{43}$$

$$\overleftrightarrow{\boldsymbol{\mathcal{P}}}_3\boldsymbol{q} = (-q_3,q_2,-q_1,q_0)^T. \tag{44}$$

If the Hamiltonian is decomposed so that each partial Hamiltonian may not have a conjugate pair of a coordinate and momentum, the symplectic integrator will be straightforwardly obtained. In the case that the partial Hamiltonian has to have coupled conjugate variables, it is not always guaranteed to yield a symplectic integrator. This is why we tried to avoid coupled variables in the partial Hamiltonians. Although there are two types of coupled variables of $\sum_{i=1}^{N}(\boldsymbol{\pi}_i'^T\overleftrightarrow{\boldsymbol{\mathcal{P}}}_k\boldsymbol{q}_i)^2/8I_k s^2$, where $k=0,1,\ldots,3$, and $sP_s^2/2Q$ (the pair of $\boldsymbol{q}_i$ and $\boldsymbol{\pi}'$ and that of s and P_s are the coupled conjugate variables), the corresponding symplectic integrators can also be obtained as described below. In the limit of $I_0\to\infty$, $H_{\text{NP-RB0}}$ goes to zero: $H_{\text{NP-RB0}}\to 0$. Hereafter, then only Hamiltonians from $H_{\text{NP-RB1}}$ to $H_{\text{NP-RB5}}$ are considered. The second-order formula with respect to Δt is obtained by the decomposition of the time propagator $\exp[D\Delta t]$ into a product of five time propagators:

$$\begin{aligned}\exp[D\Delta t] = {}& \exp\left[D_5\frac{\Delta t}{2}\right]\exp\left[D_4\frac{\Delta t}{2}\right]\exp\left[D_3\frac{\Delta t}{2}\right]\\ &\times\exp\left[D_2\frac{\Delta t}{2}\right]\exp[D_1\Delta t]\exp\left[D_2\frac{\Delta t}{2}\right]\\ &\times\exp\left[D_3\frac{\Delta t}{2}\right]\exp\left[D_4\frac{\Delta t}{2}\right]\exp\left[D_5\frac{\Delta t}{2}\right]\\ &+O((\Delta)^3).\end{aligned} \tag{45}$$

Higher-order formulas can also be obtained in a similar manner. The explicit form of each operator is as follows:

$$\begin{aligned}D_1 = {}& \sum_{i=1}^{N}\left(\frac{\partial H_{\text{NP-RB1}}}{\partial \boldsymbol{p}_i}\cdot\frac{\partial}{\partial \boldsymbol{r}_i} - \frac{\partial H_{\text{NP-RB1}}}{\partial \boldsymbol{r}_i}\cdot\frac{\partial}{\partial \boldsymbol{p}_i'}\right) + \sum_{i=1}^{N}\left(\frac{\partial H_{\text{NP-RB1}}}{\partial \boldsymbol{\pi}_i}\cdot\frac{\partial}{\partial \boldsymbol{q}_i} - \frac{\partial H_{\text{NP-RB1}}}{\partial \boldsymbol{q}_i}\cdot\frac{\partial}{\partial \boldsymbol{\pi}_i}\right) + \frac{\partial H_{\text{NP-RB1}}}{\partial P_s}\frac{\partial}{\partial s} - \frac{\partial H_{\text{NP-RB1}}}{\partial s}\frac{\partial}{\partial P_s}\\ = {}& \sum_{i=1}^{N}\frac{\boldsymbol{p}_i'}{m_i s}\cdot\frac{\partial}{\partial \boldsymbol{r}_i} + \sum_{i=1}^{N}\frac{1}{4I_1 s}(\boldsymbol{\pi}_i'^T\overleftrightarrow{\boldsymbol{\mathcal{P}}}_1\boldsymbol{q}_i)(\overleftrightarrow{\boldsymbol{\mathcal{P}}}_1\boldsymbol{q}_i)\cdot\frac{\partial}{\partial \boldsymbol{q}_i} + \sum_{i=1}^{N}\frac{1}{4I_1 s}(\boldsymbol{\pi}_i'^T\overleftrightarrow{\boldsymbol{\mathcal{P}}}_1\boldsymbol{q}_i)(\overleftrightarrow{\boldsymbol{\mathcal{P}}}_1\boldsymbol{\pi}_i')\cdot\frac{\partial}{\partial \boldsymbol{\pi}_i'}\\ &+\left[\sum_{i=1}^{N}\frac{\boldsymbol{p}_i'^2}{2m_i s^2} + \sum_{i=1}^{N}\frac{1}{8I_1 s^2}(\boldsymbol{\pi}_i'^T\overleftrightarrow{\boldsymbol{\mathcal{P}}}_1\boldsymbol{q}_i)^2 - gk_BT_0\log s + H_0 - gk_BT_0\right]\frac{\partial}{\partial P_s},\end{aligned} \tag{46}$$

$$D_2 = \sum_{i=1}^{N}\frac{1}{4I_2 s}(\boldsymbol{\pi}_i'^T\overleftrightarrow{\boldsymbol{\mathcal{P}}}_2\boldsymbol{q}_i)(\overleftrightarrow{\boldsymbol{\mathcal{P}}}_2\boldsymbol{q}_i)\cdot\frac{\partial}{\partial \boldsymbol{q}_i} + \sum_{i=1}^{N}\frac{1}{4I_2 s}(\boldsymbol{\pi}_i'^T\overleftrightarrow{\boldsymbol{\mathcal{P}}}_2\boldsymbol{q}_i)(\overleftrightarrow{\boldsymbol{\mathcal{P}}}_2\boldsymbol{\pi}_i')\cdot\frac{\partial}{\partial \boldsymbol{\pi}_i'} + \left[\sum_{i=1}^{N}\frac{1}{8I_2 s^2}(\boldsymbol{\pi}_i'^T\overleftrightarrow{\boldsymbol{\mathcal{P}}}_2\boldsymbol{q}_i)^2\right]\frac{\partial}{\partial P_s}, \tag{47}$$

$$D_3 = \sum_{i=1}^{N}\frac{1}{4I_3 s}(\boldsymbol{\pi}_i'^T\overleftrightarrow{\boldsymbol{\mathcal{P}}}_3\boldsymbol{q}_i)(\overleftrightarrow{\boldsymbol{\mathcal{P}}}_3\boldsymbol{q}_i)\cdot\frac{\partial}{\partial \boldsymbol{q}_i} + \sum_{i=1}^{N}\frac{1}{4I_3 s}(\boldsymbol{\pi}_i'^T\overleftrightarrow{\boldsymbol{\mathcal{P}}}_3\boldsymbol{q}_i)(\overleftrightarrow{\boldsymbol{\mathcal{P}}}_3\boldsymbol{\pi}_i')\cdot\frac{\partial}{\partial \boldsymbol{\pi}_i'} + \left[\sum_{i=1}^{N}\frac{1}{8I_3 s^2}(\boldsymbol{\pi}_i'^T\overleftrightarrow{\boldsymbol{\mathcal{P}}}_3\boldsymbol{q}_i)^2\right]\frac{\partial}{\partial P_s}, \tag{48}$$

$$D_4 = \sum_{i=1}^{N}s\boldsymbol{F}_i\cdot\frac{\partial}{\partial \boldsymbol{p}_i'} + \sum_{i=1}^{N}2s(\overleftrightarrow{\boldsymbol{S}}(\boldsymbol{q}_i)\boldsymbol{N}_i^{(4)})\cdot\frac{\partial}{\partial \boldsymbol{\pi}_i'} - E(\boldsymbol{r}^{\{N\}},\boldsymbol{q}^{\{N\}})\frac{\partial}{\partial P_s}, \tag{49}$$

$$D_5 = \frac{sP_s}{Q}\frac{\partial}{\partial s} - \frac{P_s^2}{2Q}\frac{\partial}{\partial P_s}. \tag{50}$$

There is no term higher than the second power of Δt in the time developments by D_4, because there is no conjugate pair in $H_{\text{NP-RB4}}$. Although there is a conjugate pair of $\boldsymbol{q}_i$ and $\boldsymbol{\pi}_i'$ in $H_{\text{NP-RB1}}$, the time developments of $\boldsymbol{q}_i$ and $\boldsymbol{\pi}_i'$ by $H_{\text{NP-RB1}}$ are given by[5]

$$\exp[D_1\Delta t]\boldsymbol{q}_i = \cos(\zeta_{i1}\Delta t)\boldsymbol{q}_i + \sin(\zeta_{i1}\Delta t)\overleftrightarrow{\boldsymbol{\mathcal{P}}}_1\boldsymbol{q}_i, \tag{51}$$

$$\exp[D_1\Delta t]\boldsymbol{\pi}_i' = \cos(\zeta_{i1}\Delta t)\boldsymbol{\pi}_i' + \sin(\zeta_{i1}\Delta t)\overleftrightarrow{\boldsymbol{\mathcal{P}}}_1\boldsymbol{\pi}_i', \tag{52}$$

where

$$\zeta_{i1} = \frac{1}{4I_1 s}\boldsymbol{\pi}_i'^T\overleftrightarrow{\boldsymbol{\mathcal{P}}}_1\boldsymbol{q}_i. \tag{53}$$

The time developments of $\boldsymbol{q}_i$ and $\boldsymbol{\pi}_i'$ by D_2 and D_3 are also obtained in the same way. Although there is another conjugate pair of s and P_s in $H_{\text{NP-RB5}}$, the time developments of s and P_s by D_5 are given explicitly by[12]

$$\exp[D_5\Delta t]s = s\left(1 + \frac{P_s}{2Q}\Delta t\right)^2, \tag{54}$$

$$\exp[D_5\Delta t]P_s = P_s \Big/ \left(1 + \frac{P_s}{2Q}\Delta t\right). \tag{55}$$

Finally, the explicit symplectic time developments for rigid-body molecules in the canonical ensemble is obtained from Eq. (45). Here, a symbol of $\leftarrow$ stands for a substitution in a computer program (i.e., the variables in each step adopt the substitutions in the preceding steps).

Step 1. $\exp[D_5\Delta t/2]$ operation:

$$s \leftarrow s\left(1 + \frac{P_s}{2Q}\frac{\Delta t}{2}\right)^2, \tag{56}$$

$$P_s \leftarrow P_s \Big/ \left(1 + \frac{P_s}{2Q}\frac{\Delta t}{2}\right). \tag{57}$$

Step 2. $\exp[D_4\Delta t/2]$ operation:

$$\boldsymbol{p}_i' \leftarrow \boldsymbol{p}_i' + s\boldsymbol{F}_i\frac{\Delta t}{2}, \tag{58}$$

$$\boldsymbol{\pi}_i' \leftarrow \boldsymbol{\pi}_i' + 2s\overleftrightarrow{\boldsymbol{S}}(\boldsymbol{q}_i)\boldsymbol{N}_i^{(4)}\frac{\Delta t}{2}, \tag{59}$$

$$P_s \leftarrow P_s - E(\boldsymbol{r}^{\{N\}},\boldsymbol{q}^{\{N\}})\frac{\Delta t}{2}. \tag{60}$$

Step 3. $\exp[D_3\Delta t/2]$ operation:

$$\zeta_{i3} \leftarrow \frac{1}{4I_3 s}\boldsymbol{\pi}_i'^T\overleftrightarrow{\boldsymbol{\mathcal{P}}}_3\boldsymbol{q}_i, \tag{61}$$

$$\boldsymbol{q}_i \leftarrow \cos\left(\zeta_{i3}\frac{\Delta t}{2}\right)\boldsymbol{q}_i + \sin\left(\zeta_{i3}\frac{\Delta t}{2}\right)\overleftrightarrow{\boldsymbol{\mathcal{P}}}_3\boldsymbol{q}_i, \tag{62}$$

$$\boldsymbol{\pi}_i' \leftarrow \cos\left(\zeta_{i3}\frac{\Delta t}{2}\right)\boldsymbol{\pi}_i' + \sin\left(\zeta_{i3}\frac{\Delta t}{2}\right)\overleftrightarrow{\boldsymbol{\mathcal{P}}}_3\boldsymbol{\pi}_i', \tag{63}$$

$$P_s \leftarrow P_s + \left(\sum_{i=1}^{N} 2I_3\zeta_{i3}^2\right)\frac{\Delta t}{2}. \tag{64}$$

Step 4. $\exp[D_2\Delta t/2]$ operation:

$$\zeta_{i2} \leftarrow \frac{1}{4I_2 s}\boldsymbol{\pi}_i'^T\overleftrightarrow{\boldsymbol{\mathcal{P}}}_2\boldsymbol{q}_i, \tag{65}$$

$$\boldsymbol{q}_i \leftarrow \cos\left(\zeta_{i2}\frac{\Delta t}{2}\right)\boldsymbol{q}_i + \sin\left(\zeta_{i2}\frac{\Delta t}{2}\right)\overleftrightarrow{\boldsymbol{\mathcal{P}}}_2\boldsymbol{q}_i, \tag{66}$$

$$\boldsymbol{\pi}_i' \leftarrow \cos\left(\zeta_{i2}\frac{\Delta t}{2}\right)\boldsymbol{\pi}_i' + \sin\left(\zeta_{i2}\frac{\Delta t}{2}\right)\overleftrightarrow{\boldsymbol{\mathcal{P}}}_2\boldsymbol{\pi}_i', \tag{67}$$

$$P_s \leftarrow P_s + \left(\sum_{i=1}^{N} 2I_2\zeta_{i2}^2\right)\frac{\Delta t}{2}. \tag{68}$$

Step 5. $\exp[D_1\Delta t]$ operation:

$$\boldsymbol{r}_i \leftarrow \boldsymbol{r}_i + \frac{\boldsymbol{p}_i'}{m_i s}\Delta t, \tag{69}$$

$$\zeta_{i1} \leftarrow \frac{1}{4I_1 s}\boldsymbol{\pi}_i'^T\overleftrightarrow{\boldsymbol{\mathcal{P}}}_1\boldsymbol{q}_i, \tag{70}$$

$$\boldsymbol{q}_i \leftarrow \cos(\zeta_{i1}\Delta t)\boldsymbol{q}_i + \sin(\zeta_{i1}\Delta t)\overleftrightarrow{\boldsymbol{\mathcal{P}}}_1\boldsymbol{q}_i, \tag{71}$$

$$\boldsymbol{\pi}_i' \leftarrow \cos(\zeta_{i1}\Delta t)\boldsymbol{\pi}_i' + \sin(\zeta_{i1}\Delta t)\overleftrightarrow{\boldsymbol{\mathcal{P}}}_1\boldsymbol{\pi}_i', \tag{72}$$

$$P_s \leftarrow P_s + \left(\sum_{i=1}^{N}\frac{\boldsymbol{p}_i'^2}{2m_i s^2} + \sum_{i=1}^{N} 2I_1\zeta_{i1}^2 - gk_BT_0\log s + H_0 - gk_BT_0\right)\Delta t. \tag{73}$$

Step 6. $\exp[D_2\Delta t/2]$ operation:

$$\zeta_{i2} \leftarrow \frac{1}{4I_2 s}\boldsymbol{\pi}_i'^T\overleftrightarrow{\boldsymbol{\mathcal{P}}}_2\boldsymbol{q}_i, \tag{74}$$

$$\boldsymbol{q}_i \leftarrow \cos\left(\zeta_{i2}\frac{\Delta t}{2}\right)\boldsymbol{q}_i + \sin\left(\zeta_{i2}\frac{\Delta t}{2}\right)\overleftrightarrow{\boldsymbol{\mathcal{P}}}_2\boldsymbol{q}_i, \tag{75}$$

$$\boldsymbol{\pi}_i' \leftarrow \cos\left(\zeta_{i2}\frac{\Delta t}{2}\right)\boldsymbol{\pi}_i' + \sin\left(\zeta_{i2}\frac{\Delta t}{2}\right)\overleftrightarrow{\boldsymbol{\mathcal{P}}}_2\boldsymbol{\pi}_i', \tag{76}$$

$$P_s \leftarrow P_s + \left(\sum_{i=1}^{N} 2I_2\zeta_{i2}^2\right)\frac{\Delta t}{2}. \tag{77}$$

Step 7. $\exp[D_3\Delta t/2]$ operation:

$$\zeta_{i3} \leftarrow \frac{1}{4I_3 s}\boldsymbol{\pi}_i'^T\overleftrightarrow{\boldsymbol{\mathcal{P}}}_3\boldsymbol{q}_i, \tag{78}$$

$$\boldsymbol{q}_i \leftarrow \cos\left(\zeta_{i3}\frac{\Delta t}{2}\right)\boldsymbol{q}_i + \sin\left(\zeta_{i3}\frac{\Delta t}{2}\right)\overleftrightarrow{\mathcal{P}}_3\boldsymbol{q}_i, \tag{79}$$

$$\boldsymbol{\pi}_i' \leftarrow \cos\left(\zeta_{i3}\frac{\Delta t}{2}\right)\boldsymbol{\pi}_i' + \sin\left(\zeta_{i3}\frac{\Delta t}{2}\right)\overleftrightarrow{\mathcal{P}}_3\boldsymbol{\pi}_i', \tag{80}$$

$$P_s \leftarrow P_s + \left(\sum_{i=1}^{N} 2I_3\zeta_{i3}^2\right)\frac{\Delta t}{2}. \tag{81}$$

Step 8. $\exp[D_4\Delta t/2]$ operation:

$$\boldsymbol{p}_i' \leftarrow \boldsymbol{p}_i' + s\boldsymbol{F}_i\frac{\Delta t}{2}, \tag{82}$$

$$\boldsymbol{\pi}_i' \leftarrow \boldsymbol{\pi}_i' + 2s\overleftrightarrow{\boldsymbol{S}}(\boldsymbol{q}_i)\boldsymbol{N}_i^{(4)}\frac{\Delta t}{2}, \tag{83}$$

$$P_s \leftarrow P_s - E(\boldsymbol{r}^{\{N\}},\boldsymbol{q}^{\{N\}})\frac{\Delta t}{2}. \tag{84}$$

Step 9. $\exp[D_5\Delta t/2]$ operation:

$$s \leftarrow s\left(1 + \frac{P_s}{2Q}\frac{\Delta t}{2}\right)^2, \tag{85}$$

$$P_s \leftarrow P_s \Big/ \left(1 + \frac{P_s}{2Q}\frac{\Delta t}{2}\right). \tag{86}$$

D. Symplectic molecular dynamics algorithm for rigid-body molecules combined with the Nosé-Poincaré thermostat and the Andersen barostat

In this section we present the explicit symplectic MD algorithm for rigid-body molecules in the isobaric-isothermal ensemble. The Hamiltonian for rigid-body molecules at temperature T_0 and pressure P_0 is given by combining the Hamiltonian in Eq. (23) and the Andersen barostat[17] as follows:

$$\begin{aligned} H_{\text{NPA-RB}} = s\Bigg[&\sum_{i=1}^{N}\frac{\tilde{\boldsymbol{p}}_i^2}{2m_i s^2 V^{2/3}} + \sum_{i=1}^{N}\frac{1}{8s^2}\boldsymbol{\pi}_i'^T\overleftrightarrow{\boldsymbol{S}}(\boldsymbol{q}_i)\overleftrightarrow{\boldsymbol{D}}_i\overleftrightarrow{\boldsymbol{S}}^T(\boldsymbol{q}_i)\boldsymbol{\pi}_i' \\ &+ E(\tilde{\boldsymbol{r}}^{\{N\}},\boldsymbol{q}^{\{N\}},V) + \frac{P_s^2}{2Q} + gk_BT_0\log s + \frac{P_V^2}{2W} \\ &+ P_0V - H_0\Bigg] \\ = s[&H_{\text{NA}}(\tilde{\boldsymbol{r}}^{\{N\}},\tilde{\boldsymbol{p}}^{\{N\}},\boldsymbol{q}^{\{N\}},\boldsymbol{\pi}'^{\{N\}},s,P_s,V,P_V) - H_0], \end{aligned} \tag{87}$$

where $\tilde{\boldsymbol{p}}_i$ and $\tilde{\boldsymbol{r}}_i$ are the scaled momentum and the scaled coordinate by volume V and the degree of the Nosé-Poincaré thermostat s. They are related to $\boldsymbol{p}_i$ and $\boldsymbol{r}_i$ by

$$\boldsymbol{p}_i = \frac{\tilde{\boldsymbol{p}}_i}{sV^{1/3}}, \tag{88}$$

$$\boldsymbol{r}_i = V^{1/3}\tilde{\boldsymbol{r}}_i. \tag{89}$$

The constant W is the "mass" associated with V. The variable P_V is the conjugate momenta for V. The constant H_0 here is the initial value of the Nosé-Andersen Hamiltonian H_{NA}. The equations of motion are given by

$$\dot{\boldsymbol{r}}_i = \frac{\boldsymbol{p}_i}{m_i} + \frac{\dot{V}}{3V}\boldsymbol{r}_i, \tag{90}$$

$$\dot{\boldsymbol{p}}_i = \boldsymbol{F}_i - \left(\frac{\dot{s}}{s} + \frac{\dot{V}}{3V}\right)\boldsymbol{p}_i, \tag{91}$$

$$\dot{\boldsymbol{q}}_i = \frac{1}{2}\overleftrightarrow{\boldsymbol{S}}(\boldsymbol{q}_i)\boldsymbol{\omega}_i^{(4)}, \tag{92}$$

$$\overleftrightarrow{\boldsymbol{I}}_i\dot{\boldsymbol{\omega}}_i = \boldsymbol{N}_i - \boldsymbol{\omega}_i \times (\overleftrightarrow{\boldsymbol{I}}_i\boldsymbol{\omega}_i) - \frac{\dot{s}}{s}\overleftrightarrow{\boldsymbol{I}}_i\boldsymbol{\omega}_i, \tag{93}$$

$$\dot{s} = s\frac{P_s}{Q}, \tag{94}$$

$$\dot{P}_s = \sum_{i=1}^{N}\frac{\boldsymbol{p}_i^2}{m_i} + \sum_{i=1}^{N}\boldsymbol{\omega}_i^T\overleftrightarrow{\boldsymbol{I}}_i\boldsymbol{\omega}_i - gk_BT_0, \tag{95}$$

$$\dot{V} = s\frac{P_V}{W}, \tag{96}$$

$$\dot{P}_V = s\left[\frac{1}{3V}\left(\sum_{i=1}^{N}\frac{\boldsymbol{p}_i^2}{m_i} + \sum_{i=1}^{N}\boldsymbol{F}_i\cdot\boldsymbol{r}_i\right) - P_0\right], \tag{97}$$

where the relation of

$$H_{\text{NA}} - H_0 = 0 \tag{98}$$

is used.

The Hamiltonian in the isobaric-isothermal ensemble is separated into six terms as follows:

$$\begin{aligned} H_{\text{NPA-RB}} = &H_{\text{NPA-RB1}} + H_{\text{NPA-RB2}} + H_{\text{NPA-RB3}} + H_{\text{NPA-RB4}} \\ &+ H_{\text{NPA-RB5}} + H_{\text{NPA-RB6}}, \end{aligned} \tag{99}$$

$$\begin{aligned} H_{\text{NPA-RB1}} = s\Bigg[&\sum_{i=1}^{N}\frac{\tilde{\boldsymbol{p}}_i^2}{2m_i s^2 V^{2/3}} + \sum_{i=1}^{N}\frac{1}{8I_1 s^2}(\boldsymbol{\pi}_i'^T\overleftrightarrow{\mathcal{P}}_1\boldsymbol{q}_i)^2 \\ &+ gk_BT_0\log s - H_0\Bigg], \end{aligned} \tag{100}$$

$$H_{\text{NPA-RB2}} = s\sum_{i=1}^{N}\frac{1}{8I_2 s^2}(\boldsymbol{\pi}_i'^T\overleftrightarrow{\mathcal{P}}_2\boldsymbol{q}_i)^2, \tag{101}$$

$$H_{\text{NPA-RB3}} = s\sum_{i=1}^{N} \frac{1}{8I_3 s^2}(\boldsymbol{\pi}_i'^T \overleftrightarrow{\mathcal{P}}_3 \boldsymbol{q}_i)^2, \tag{102}$$

$$H_{\text{NPA-RB4}} = s\frac{P_V^2}{2W}, \tag{103}$$

$$H_{\text{NPA-RB5}} = s[E(\tilde{\boldsymbol{r}}^{\{N\}}, \boldsymbol{q}^{\{N\}}, V) + P_0 V], \tag{104}$$

$$H_{\text{NPA-RB6}} = s\frac{P_s^2}{2Q}, \tag{105}$$

where the term of $s\Sigma_{i=1}^{N}(\boldsymbol{\pi}_i'^T \overleftrightarrow{\mathcal{P}}_0 \boldsymbol{q}_i)^2/8I_0 s^2$ has been neglected again because it is zero in the limit of $I_0 \to \infty$. As in the decomposition in Eq. (45) in the canonical ensemble, the second-order formula is obtained for the time propagator $\exp[D\Delta t]$ as a product of six time propagators:

$$\exp[D\Delta t] = \exp\left[D_6\frac{\Delta t}{2}\right]\exp\left[D_5\frac{\Delta t}{2}\right]\exp\left[D_4\frac{\Delta t}{2}\right]\exp\left[D_3\frac{\Delta t}{2}\right]\exp\left[D_2\frac{\Delta t}{2}\right]\exp[D_1\Delta t]\exp\left[D_2\frac{\Delta t}{2}\right]$$
$$\times \exp\left[D_3\frac{\Delta t}{2}\right]\exp\left[D_4\frac{\Delta t}{2}\right]\exp\left[D_5\frac{\Delta t}{2}\right]\exp\left[D_6\frac{\Delta t}{2}\right] + O((\Delta t)^3), \tag{106}$$

where $D_1, D_2, \ldots, D_6$ are the time propagators which correspond to $H_{\text{NPA-RB1}}, H_{\text{NPA-RB2}}, \ldots, H_{\text{NPA-RB6}}$, respectively.

According to the decomposition in Eq. (106), the explicit symplectic time developments for rigid-body molecules in the isobaric-isothermal ensemble are given as follows:

Step 1. $\exp[D_6\Delta t/2]$ operation:

$$s \leftarrow s\left(1 + \frac{P_s}{2Q}\frac{\Delta t}{2}\right)^2, \tag{107}$$

$$P_s \leftarrow P_s \Big/ \left(1 + \frac{P_s}{2Q}\frac{\Delta t}{2}\right). \tag{108}$$

Step 2. $\exp[D_5\Delta t/2]$ operation:

$$\tilde{\boldsymbol{p}}_i \leftarrow \tilde{\boldsymbol{p}}_i + sV^{1/3}\boldsymbol{F}_i\frac{\Delta t}{2}, \tag{109}$$

$$\boldsymbol{\pi}_i' \leftarrow \boldsymbol{\pi}_i' + 2s\overleftrightarrow{S}(\boldsymbol{q}_i)N_i^{(4)}\frac{\Delta t}{2}, \tag{110}$$

$$P_s \leftarrow P_s - [E(\tilde{\boldsymbol{r}}^{\{N\}}, \boldsymbol{q}^{\{N\}}, V) + P_0 V]\frac{\Delta t}{2}, \tag{111}$$

$$P_V \leftarrow P_V + s\left(\frac{1}{3V}\sum_{i=1}^{N}\boldsymbol{F}_i \cdot \boldsymbol{r}_i - P_0\right)\frac{\Delta t}{2}. \tag{112}$$

Step 3. $\exp[D_4\Delta t/2]$ operation:

$$P_s \leftarrow P_s - \frac{P_V^2}{2W}\frac{\Delta t}{2}, \tag{113}$$

$$V \leftarrow V + s\frac{P_V}{W}\frac{\Delta t}{2}. \tag{114}$$

Step 4. $\exp[D_3\Delta t/2]$ operation:

$$\zeta_{i3} \leftarrow \frac{1}{4I_3 s}\boldsymbol{\pi}_i'^T \overleftrightarrow{\mathcal{P}}_3 \boldsymbol{q}_i, \tag{115}$$

$$\boldsymbol{q}_i \leftarrow \cos\left(\zeta_{i3}\frac{\Delta t}{2}\right)\boldsymbol{q}_i + \sin\left(\zeta_{i3}\frac{\Delta t}{2}\right)\overleftrightarrow{\mathcal{P}}_3 \boldsymbol{q}_i, \tag{116}$$

$$\boldsymbol{\pi}_i' \leftarrow \cos\left(\zeta_{i3}\frac{\Delta t}{2}\right)\boldsymbol{\pi}_i' + \sin\left(\zeta_{i3}\frac{\Delta t}{2}\right)\overleftrightarrow{\mathcal{P}}_3 \boldsymbol{\pi}_i', \tag{117}$$

$$P_s \leftarrow P_s + \left(\sum_{i=1}^{N} 2I_3\zeta_{i3}^2\right)\frac{\Delta t}{2}. \tag{118}$$

Step 5. $\exp[D_2\Delta t/2]$ operation:

$$\zeta_{i2} \leftarrow \frac{1}{4I_2 s}\boldsymbol{\pi}_i'^T \overleftrightarrow{\mathcal{P}}_2 \boldsymbol{q}_i, \tag{119}$$

$$\boldsymbol{q}_i \leftarrow \cos\left(\zeta_{i2}\frac{\Delta t}{2}\right)\boldsymbol{q}_i + \sin\left(\zeta_{i2}\frac{\Delta t}{2}\right)\overleftrightarrow{\mathcal{P}}_2 \boldsymbol{q}_i, \tag{120}$$

$$\boldsymbol{\pi}_i' \leftarrow \cos\left(\zeta_{i2}\frac{\Delta t}{2}\right)\boldsymbol{\pi}_i' + \sin\left(\zeta_{i2}\frac{\Delta t}{2}\right)\overleftrightarrow{\mathcal{P}}_2 \boldsymbol{\pi}_i', \tag{121}$$

$$P_s \leftarrow P_s + \left(\sum_{i=1}^{N} 2I_2\zeta_{i2}^2\right)\frac{\Delta t}{2}. \tag{122}$$

Step 6. $\exp[D_1\Delta t]$ operation:

$$\tilde{\boldsymbol{r}}_i \leftarrow \tilde{\boldsymbol{r}}_i + \frac{\tilde{\boldsymbol{p}}_i}{m_i s V^{2/3}}\Delta t, \tag{123}$$

$$\zeta_{i1} \leftarrow \frac{1}{4I_1 s}\boldsymbol{\pi}_i'^T \overleftrightarrow{\mathcal{P}}_1 \boldsymbol{q}_i, \tag{124}$$

$$\boldsymbol{q}_i \leftarrow \cos(\zeta_{i1}\Delta t)\boldsymbol{q}_i + \sin(\zeta_{i1}\Delta t)\overleftrightarrow{\mathcal{P}}_1 \boldsymbol{q}_i, \tag{125}$$

$$\boldsymbol{\pi}_i' \leftarrow \cos(\zeta_{i1}\Delta t)\boldsymbol{\pi}_i' + \sin(\zeta_{i1}\Delta t)\overleftrightarrow{\mathcal{P}}_1 \boldsymbol{\pi}_i', \tag{126}$$

$$P_s \leftarrow P_s + \left(\sum_{i=1}^{N} \frac{\tilde{\boldsymbol{p}}_i^2}{2m_i s^2 V^{2/3}} + \sum_{i=1}^{N} 2I_1 \zeta_{i1}^2 - gk_B T_0 \log s + H_0 - gk_B T_0 \right) \Delta t. \tag{127}$$

$$P_V \leftarrow P_V + \sum_{i=1}^{N} \frac{\tilde{\boldsymbol{p}}_i^2}{3m_i s V^{5/3}} \Delta t. \tag{128}$$

Step 7. $\exp[D_2 \Delta t/2]$ operation:

$$\zeta_{i2} \leftarrow \frac{1}{4I_2 s} \boldsymbol{\pi}_i'^T \overleftrightarrow{\boldsymbol{\mathcal{P}}}_2 \boldsymbol{q}_i, \tag{129}$$

$$\boldsymbol{q}_i \leftarrow \cos\left(\zeta_{i2} \frac{\Delta t}{2} \right) \boldsymbol{q}_i + \sin\left(\zeta_{i2} \frac{\Delta t}{2} \right) \overleftrightarrow{\boldsymbol{\mathcal{P}}}_2 \boldsymbol{q}_i, \tag{130}$$

$$\boldsymbol{\pi}_i' \leftarrow \cos\left(\zeta_{i2} \frac{\Delta t}{2} \right) \boldsymbol{\pi}_i' + \sin\left(\zeta_{i2} \frac{\Delta t}{2} \right) \overleftrightarrow{\boldsymbol{\mathcal{P}}}_2 \boldsymbol{\pi}_i', \tag{131}$$

$$P_s \leftarrow P_s + \left(\sum_{i=1}^{N} 2I_2 \zeta_{i2}^2 \right) \frac{\Delta t}{2}. \tag{132}$$

Step 8. $\exp[D_3 \Delta t/2]$ operation:

$$\zeta_{i3} \leftarrow \frac{1}{4I_3 s} \boldsymbol{\pi}_i'^T \overleftrightarrow{\boldsymbol{\mathcal{P}}}_3 \boldsymbol{q}_i, \tag{133}$$

$$\boldsymbol{q}_i \leftarrow \cos\left(\zeta_{i3} \frac{\Delta t}{2} \right) \boldsymbol{q}_i + \sin\left(\zeta_{i3} \frac{\Delta t}{2} \right) \overleftrightarrow{\boldsymbol{\mathcal{P}}}_3 \boldsymbol{q}_i, \tag{134}$$

$$\boldsymbol{\pi}_i' \leftarrow \cos\left(\zeta_{i3} \frac{\Delta t}{2} \right) \boldsymbol{\pi}_i' + \sin\left(\zeta_{i3} \frac{\Delta t}{2} \right) \overleftrightarrow{\boldsymbol{\mathcal{P}}}_3 \boldsymbol{\pi}_i', \tag{135}$$

$$P_s \leftarrow P_s + \left(\sum_{i=1}^{N} 2I_3 \zeta_{i3}^2 \right) \frac{\Delta t}{2}. \tag{136}$$

Step 9. $\exp[D_4 \Delta t/2]$ operation:

$$P_s \leftarrow P_s - \frac{P_V^2}{2W} \frac{\Delta t}{2}, \tag{137}$$

$$V \leftarrow V + s \frac{P_V}{W} \frac{\Delta t}{2}. \tag{138}$$

Step 10. $\exp[D_5 \Delta t/2]$ operation:

$$\tilde{\boldsymbol{p}}_i \leftarrow \tilde{\boldsymbol{p}}_i + sV^{1/3} \boldsymbol{F}_i \frac{\Delta t}{2}, \tag{139}$$

$$\boldsymbol{\pi}_i' \leftarrow \boldsymbol{\pi}_i' + 2s \overleftrightarrow{\boldsymbol{S}}(\boldsymbol{q}_i) N_i^{(4)} \frac{\Delta t}{2}, \tag{140}$$

$$P_s \leftarrow P_s - [E(\tilde{\boldsymbol{r}}^{\{N\}}, \boldsymbol{q}^{\{N\}}, V) + P_0 V] \frac{\Delta t}{2}, \tag{141}$$

$$P_V \leftarrow P_V + s \left(\frac{1}{3V} \sum_{i=1}^{N} \boldsymbol{F}_i \cdot \boldsymbol{r}_i - P_0 \right) \frac{\Delta t}{2}. \tag{142}$$

Step 11. $\exp[D_6 \Delta t/2]$ operation:

$$s \leftarrow s \left(1 + \frac{P_s}{2Q} \frac{\Delta t}{2} \right)^2, \tag{143}$$

$$P_s \leftarrow P_s \Big/ \left(1 + \frac{P_s}{2Q} \frac{\Delta t}{2} \right). \tag{144}$$

E. Symplectic molecular dynamics algorithm for rigid-body molecules in the constant temperature, constant normal pressure, and constant lateral surface area ensemble

An explicit symplectic MD algorithm in the constant temperature, constant normal pressure, and constant lateral surface area ensemble is also easily obtained. In Sec. II D Andersen's constant pressure algorithm was employed for all three side lengths of the simulation cell. On the other hand, one of the side lengths of the simulation cell fluctuates in the constant normal pressure and constant lateral surface area ensemble. This ensemble is often used for membrane systems.[16] The Hamiltonian for this ensemble is given by

$$H_{\text{NPA1-RB}} = s \Bigg[\sum_{i=1}^{N} \frac{\tilde{p}_{xi}^2}{2m_i s^2 L^2} + \sum_{i=1}^{N} \frac{p_{yi}'^2 + p_{zi}'^2}{2m_i s^2} + \sum_{i=1}^{N} \frac{1}{8s^2} \boldsymbol{\pi}_i'^T \overleftrightarrow{\boldsymbol{S}}(\boldsymbol{q}_i) \overleftrightarrow{\boldsymbol{D}}_i \overleftrightarrow{\boldsymbol{S}}^T(\boldsymbol{q}_i) \boldsymbol{\pi}_i' + E(\tilde{x}^{\{N\}}, y^{\{N\}}, z^{\{N\}}, \boldsymbol{q}^{\{N\}}, L) + \frac{P_s^2}{2Q} + gk_B T_0 \log s + \frac{P_L^2}{2W} + P_0 AL - H_0 \Bigg], \tag{145}$$

where the variable P_L is the conjugate momenta for the side length L of the simulation cell along the x axis. The constant A is the lateral surface area on the yz plane. Therefore the volume of the simulation cell V is given by AL. Note that x components of $\boldsymbol{p}_i$ and $\boldsymbol{r}_i$ are scaled by $p_{xi} = \tilde{p}_{xi}/sL$ and $x_i = L\tilde{x}_i$, respectively, whereas y and z components of $\boldsymbol{p}_i$ are scaled by Eq. (2). The equations of motion are given by

$$\dot{x}_i = \frac{p_{xi}}{m_i} + \frac{\dot{L}}{L} x_i, \tag{146}$$

$$\dot{y}_i = \frac{p_{yi}}{m_i}, \quad \dot{z}_i = \frac{p_{zi}}{m_i}, \tag{147}$$

$$\dot{p}_{xi} = F_{xi} - \left(\frac{\dot{s}}{s} + \frac{\dot{L}}{L} \right) p_{xi}, \tag{148}$$

$$\dot{p}_{yi} = F_{yi} - \frac{\dot{s}}{s} p_{yi}, \quad \dot{p}_{zi} = F_{zi} - \frac{\dot{s}}{s} p_{zi}, \tag{149}$$

$$\dot{\boldsymbol{q}}_i = \frac{1}{2}\overleftrightarrow{\boldsymbol{S}}(\boldsymbol{q}_i)\boldsymbol{\omega}_i^{(4)}, \tag{150}$$

$$\overleftrightarrow{\boldsymbol{I}}_i\dot{\boldsymbol{\omega}}_i = \boldsymbol{N}_i - \boldsymbol{\omega}_i \times (\overleftrightarrow{\boldsymbol{I}}_i\boldsymbol{\omega}_i) - \frac{\dot{s}}{s}\overleftrightarrow{\boldsymbol{I}}_i\boldsymbol{\omega}_i, \tag{151}$$

$$\dot{s} = s\frac{P_s}{Q}, \tag{152}$$

$$\dot{P}_s = \sum_{i=1}^{N}\frac{\boldsymbol{p}_i^2}{m_i} + \sum_{i=1}^{N}\boldsymbol{\omega}_i^T\overleftrightarrow{\boldsymbol{I}}_i\boldsymbol{\omega}_i - gk_BT_0, \tag{153}$$

$$\dot{L} = s\frac{P_L}{W}, \tag{154}$$

$$\dot{P}_L = sA\left[\frac{1}{V}\left(\sum_{i=1}^{N}\frac{p_{xi}^2}{m_i} + \sum_{i=1}^{N}F_{xi}\cdot x_i\right) - P_0\right]. \tag{155}$$

The Hamiltonian in Eq. (145) is separated into six terms as follows:

$$H_{\text{NPA1-RB1}} = s\left[\sum_{i=1}^{N}\frac{\tilde{p}_{xi}^2}{2m_is^2L^2} + \sum_{i=1}^{N}\frac{p_{yi}'^2 + p_{zi}'^2}{2m_is^2} + \sum_{i=1}^{N}\frac{1}{8I_1s^2}(\boldsymbol{\pi}_i'^T\overleftrightarrow{\boldsymbol{\mathcal{P}}}_1\boldsymbol{q}_i)^2 + gk_BT_0\log s - H_0\right], \tag{156}$$

$$H_{\text{NPA1-RB2}} = s\sum_{i=1}^{N}\frac{1}{8I_2s^2}(\boldsymbol{\pi}_i'^T\overleftrightarrow{\boldsymbol{\mathcal{P}}}_2\boldsymbol{q}_i)^2, \tag{157}$$

$$H_{\text{NPA1-RB3}} = s\sum_{i=1}^{N}\frac{1}{8I_3s^2}(\boldsymbol{\pi}_i'^T\overleftrightarrow{\boldsymbol{\mathcal{P}}}_3\boldsymbol{q}_i)^2, \tag{158}$$

$$H_{\text{NPA1-RB4}} = s\frac{P_L^2}{2W}, \tag{159}$$

$$H_{\text{NPA1-RB5}} = s[E(\tilde{x}^{\{N\}}, y^{\{N\}}, z^{\{N\}}, \boldsymbol{q}^{\{N\}}, L) + P_0AL], \tag{160}$$

$$H_{\text{NPA1-RB6}} = s\frac{P_s^2}{2Q}. \tag{161}$$

In order to obtain the second-order symplectic formula, the time propagator $\exp[D\Delta t]$ is again decomposed to a product of six time propagators as in Eq. (106). The symplectic time developments are then given by

$$\exp[D_1\Delta t]\tilde{x}_i = \tilde{x}_i + \frac{\tilde{p}_{xi}}{m_isL^2}\Delta t, \tag{162}$$

$$\exp[D_1\Delta t]y_i = y_i + \frac{p_{yi}'^2}{m_is}\Delta t, \tag{163}$$

$$\exp[D_1\Delta t]z_i = z_i + \frac{p_{zi}'^2}{m_is}\Delta t, \tag{164}$$

$$\exp[D_1\Delta t]\boldsymbol{q}_i = \cos(\zeta_{i1}\Delta t)\boldsymbol{q}_i + \sin(\zeta_{i1}\Delta t)\overleftrightarrow{\boldsymbol{\mathcal{P}}}_1\boldsymbol{q}_i,$$

where

$$\zeta_{i1} = \frac{1}{4I_1s}\boldsymbol{\pi}_i'^T\overleftrightarrow{\boldsymbol{\mathcal{P}}}_1\boldsymbol{q}_i, \tag{165}$$

$$\exp[D_1\Delta t]\boldsymbol{\pi}_i' = \cos(\zeta_{i1}\Delta t)\boldsymbol{\pi}_i' + \sin(\zeta_{i1}\Delta t)\overleftrightarrow{\boldsymbol{\mathcal{P}}}_1\boldsymbol{\pi}_i', \tag{166}$$

$$\exp[D_1\Delta t]P_s = P_s + \left(\sum_{i=1}^{N}\frac{\tilde{p}_{xi}^2}{2m_is^2L^2} + \sum_{i=1}^{N}\frac{p_{yi}'^2 + p_{zi}'^2}{2m_is^2} + \sum_{i=1}^{N}2I_1\zeta_{i1}^2 - gk_BT_0\log s + H_0 - gk_BT_0\right)\Delta t, \tag{167}$$

$$\exp[D_1\Delta t]P_L = P_L + \sum_{i=1}^{N}\frac{\tilde{p}_{xi}^2}{m_isL^3}\Delta t, \tag{168}$$

$$\exp[D_2\Delta t]\boldsymbol{q}_i = \cos(\zeta_{i2}\Delta t)\boldsymbol{q}_i + \sin(\zeta_{i2}\Delta t)\overleftrightarrow{\boldsymbol{\mathcal{P}}}_2\boldsymbol{q}_i,$$

where

$$\zeta_{i2} = \frac{1}{4I_2s}\boldsymbol{\pi}_i'^T\overleftrightarrow{\boldsymbol{\mathcal{P}}}_2\boldsymbol{q}_i, \tag{169}$$

$$\exp[D_2\Delta t]\boldsymbol{\pi}_i' = \cos(\zeta_{i2}\Delta t)\boldsymbol{\pi}_i' + \sin(\zeta_{i2}\Delta t)\overleftrightarrow{\boldsymbol{\mathcal{P}}}_2\boldsymbol{\pi}_i', \tag{170}$$

$$\exp[D_2\Delta t]P_s = P_s + \left(\sum_{i=1}^{N}2I_2\zeta_{i2}^2\right)\Delta t, \tag{171}$$

$$\exp[D_3\Delta t]\boldsymbol{q}_i = \cos(\zeta_{i3}\Delta t)\boldsymbol{q}_i + \sin(\zeta_{i3}\Delta t)\overleftrightarrow{\boldsymbol{\mathcal{P}}}_3\boldsymbol{q}_i,$$

where

$$\zeta_{i3} = \frac{1}{4I_3s}\boldsymbol{\pi}_i'^T\overleftrightarrow{\boldsymbol{\mathcal{P}}}_3\boldsymbol{q}_i, \tag{172}$$

$$\exp[D_3\Delta t]\boldsymbol{\pi}_i' = \cos(\zeta_{i3}\Delta t)\boldsymbol{\pi}_i' + \sin(\zeta_{i3}\Delta t)\overleftrightarrow{\boldsymbol{\mathcal{P}}}_3\boldsymbol{\pi}_i', \tag{173}$$

$$\exp[D_3\Delta t]P_s = P_s + \left(\sum_{i=1}^{N}2I_3\zeta_{i3}^2\right)\Delta t, \tag{174}$$

$$\exp[D_4\Delta t]P_s = P_s - \frac{P_L^2}{2W}\Delta t, \tag{175}$$

$$\exp[D_4\Delta t]L = L + s\frac{P_L}{W}\Delta t, \tag{176}$$

$$\exp[D_5\Delta t]\tilde{p}_{xi} = \tilde{p}_{xi} + sLF_{xi}\Delta t, \tag{177}$$

$$\exp[D_5\Delta t]p_{yi}' = p_{yi}' + sF_{yi}\Delta t, \tag{178}$$

$$\exp[D_5\Delta t]p_{zi}' = p_{zi}' + sF_{zi}\Delta t, \tag{179}$$

$$\exp[D_5\Delta t]\boldsymbol{\pi}_i' = \boldsymbol{\pi}_i' + 2s\overleftrightarrow{\boldsymbol{S}}(\boldsymbol{q}_i)N_i^{(4)}\Delta t, \tag{180}$$

$$\exp[D_5\Delta t]P_s = P_s - (E + P_0AL)\Delta t, \tag{181}$$

$$\exp[D_5\Delta t]P_L = P_L + s\left(\frac{1}{L}\sum_{i=1}^{N} F_{xi}\cdot x_i - P_0A\right)\Delta t, \tag{182}$$

$$\exp[D_6\Delta t]s = s\left(1 + \frac{P_s}{2Q}\Delta t\right)^2, \tag{183}$$

$$\exp[D_6\Delta t]P_s = P_s \Big/ \left(1 + \frac{P_s}{2Q}\Delta t\right). \tag{184}$$

Note that Δt will be replaced in a computer program by $\Delta t/2$ for the time propagation by $D_2, D_3, \ldots, D_6$ in Eqs. (169)–(184). These time propagators are used in the order of Eq. (106).

F. Symplectic molecular dynamics algorithm for rigid-body molecules combined with the Nosé-Poincaré thermostat and the Parrinello-Rahman barostat

In this section we present an explicit symplectic MD algorithm for rigid-body molecules in the isobaric-isothermal ensemble with simulation-cell deformation. The Hamiltonian is given by combining the Hamiltonian in Eq. (23) and the Parrinello-Rahman barostat[19] as follows:

$$\begin{aligned} H_{\text{NPPR-RB}} = s\Bigg[& \sum_{i=1}^{N}\frac{1}{2m_is^2}\tilde{\boldsymbol{p}}_i^T\overleftrightarrow{\boldsymbol{G}}^{-1}\tilde{\boldsymbol{p}}_i \\ & + \sum_{i=1}^{N}\frac{1}{8s^2}\boldsymbol{\pi}_i'^T\overleftrightarrow{\boldsymbol{S}}(\boldsymbol{q}_i)\overleftrightarrow{\boldsymbol{D}}_i\overleftrightarrow{\boldsymbol{S}}^T(\boldsymbol{q}_i)\boldsymbol{\pi}_i' \\ & + E(\tilde{\boldsymbol{r}}^{\{N\}},\boldsymbol{q}^{\{N\}},\overleftrightarrow{\boldsymbol{L}}) + \frac{P_s^2}{2Q} + gk_BT_0\log s \\ & + \frac{1}{2W}\mathrm{Tr}(\overleftrightarrow{\boldsymbol{P}}_L^T\overleftrightarrow{\boldsymbol{P}}_L) + P_0V - H_0\Bigg], \end{aligned} \tag{185}$$

where $\overleftrightarrow{\boldsymbol{L}}$ is the matrix of cell parameters, $\overleftrightarrow{\boldsymbol{P}}_L$ is the conjugate momenta for $\overleftrightarrow{\boldsymbol{L}}$, and $\overleftrightarrow{\boldsymbol{G}}$ is given by $\overleftrightarrow{\boldsymbol{L}}^T\overleftrightarrow{\boldsymbol{L}}$. The scaled momentum $\tilde{\boldsymbol{p}}_i$ and the scaled coordinate $\tilde{\boldsymbol{r}}_i$ are related to $\boldsymbol{p}_i$ and $\boldsymbol{r}_i$ here by

$$\boldsymbol{p}_i = \frac{1}{s}(\overleftrightarrow{\boldsymbol{L}}^T)^{-1}\tilde{\boldsymbol{p}}_i, \tag{186}$$

$$\boldsymbol{r}_i = \overleftrightarrow{\boldsymbol{L}}\tilde{\boldsymbol{r}}_i. \tag{187}$$

The equations of motion are given by

$$\dot{\boldsymbol{r}}_i = \frac{\boldsymbol{p}_i}{m_i} + \dot{\overleftrightarrow{\boldsymbol{L}}}\overleftrightarrow{\boldsymbol{L}}^{-1}\boldsymbol{r}_i, \tag{188}$$

$$\dot{\boldsymbol{p}}_i = \boldsymbol{F}_i - \frac{\dot{s}}{s}\boldsymbol{p}_i - (\dot{\overleftrightarrow{\boldsymbol{L}}}\overleftrightarrow{\boldsymbol{L}}^{-1})^T p_i, \tag{189}$$

$$\dot{\boldsymbol{q}}_i = \frac{1}{2}\overleftrightarrow{\boldsymbol{S}}(\boldsymbol{q}_i)\boldsymbol{\omega}_i^{(4)}, \tag{190}$$

$$\overleftrightarrow{\boldsymbol{I}}_i\dot{\boldsymbol{\omega}}_i = \boldsymbol{N}_i - \boldsymbol{\omega}_i\times(\overleftrightarrow{\boldsymbol{I}}_i\boldsymbol{\omega}_i) - \frac{\dot{s}}{s}\overleftrightarrow{\boldsymbol{I}}_i\boldsymbol{\omega}_i, \tag{191}$$

$$\dot{s} = s\frac{P_s}{Q}, \tag{192}$$

$$\dot{P}_s = \sum_{i=1}^{N}\frac{\boldsymbol{p}_i^2}{m_i} + \sum_{i=1}^{N}\boldsymbol{\omega}_i^T\overleftrightarrow{\boldsymbol{I}}_i\boldsymbol{\omega}_i - gk_BT_0, \tag{193}$$

$$\dot{\overleftrightarrow{\boldsymbol{L}}} = \frac{s}{W}\overleftrightarrow{\boldsymbol{P}}_L, \tag{194}$$

$$\dot{\overleftrightarrow{\boldsymbol{P}}}_L = s\left[\frac{1}{V}\left(\sum_{i=1}^{N}\frac{1}{m_i}\boldsymbol{p}_i\boldsymbol{p}_i^T + \sum_{i=1}^{N}\boldsymbol{F}_i\boldsymbol{r}_i^T\right) - P_0\overleftrightarrow{\boldsymbol{1}}\right]\overleftrightarrow{\boldsymbol{\sigma}}, \tag{195}$$

where $\overleftrightarrow{\boldsymbol{\sigma}}$ is related to $\overleftrightarrow{\boldsymbol{L}}$ by $\overleftrightarrow{\boldsymbol{\sigma}}^T = V\overleftrightarrow{\boldsymbol{L}}^{-1}$ and $\overleftrightarrow{\boldsymbol{1}}$ is the identity matrix. Note that $\boldsymbol{p}_i\boldsymbol{p}_i^T$ and $\boldsymbol{F}_i\boldsymbol{r}_i^T$ are dyadic tensors, whose (α,β) elements $(\alpha,\beta=x,y,z)$ are $p_{\alpha i}p_{\beta i}$ and $F_{\alpha i}r_{\beta i}$, respectively. The Hamiltonian in Eq. (185) is also separated into six terms as follows:

$$\begin{aligned} H_{\text{NPPR-RB1}} = s\Bigg[& \sum_{i=1}^{N}\frac{1}{2m_is^2}\tilde{\boldsymbol{p}}_i^T\overleftrightarrow{\boldsymbol{G}}^{-1}\tilde{\boldsymbol{p}}_i + \sum_{i=1}^{N}\frac{1}{8I_1s^2}(\boldsymbol{\pi}_i'^T\overleftrightarrow{\boldsymbol{\mathcal{P}}}_1\boldsymbol{q}_i)^2 \\ & + gk_BT_0\log s - H_0\Bigg], \end{aligned} \tag{196}$$

$$H_{\text{NPPR-RB2}} = s\sum_{i=1}^{N}\frac{1}{8I_2s^2}(\boldsymbol{\pi}_i'^T\overleftrightarrow{\boldsymbol{\mathcal{P}}}_2\boldsymbol{q}_i)^2, \tag{197}$$

$$H_{\text{NPPR-RB3}} = s\sum_{i=1}^{N}\frac{1}{8I_3s^2}(\boldsymbol{\pi}_i'^T\overleftrightarrow{\boldsymbol{\mathcal{P}}}_3\boldsymbol{q}_i)^2, \tag{198}$$

$$H_{\text{NPPR-RB4}} = \frac{s}{2W}\mathrm{Tr}(\overleftrightarrow{\boldsymbol{P}}_L^T\overleftrightarrow{\boldsymbol{P}}_L), \tag{199}$$

$$H_{\text{NPPR-RB5}} = s[E(\tilde{\boldsymbol{r}}^{\{N\}},\boldsymbol{q}^{\{N\}},\overleftrightarrow{\boldsymbol{L}}) + P_0V], \tag{200}$$

$$H_{\text{NPPR-RB6}} = s\frac{P_s^2}{2Q}. \tag{201}$$

The symplectic time developments are given using the decomposition of $\exp[D\Delta t]$ in Eq. (106) by

$$\exp[D_1\Delta t]\tilde{\boldsymbol{r}}_i = \tilde{\boldsymbol{r}}_i + \frac{\Delta t}{m_is}\overleftrightarrow{\boldsymbol{G}}^{-1}\tilde{\boldsymbol{p}}_i, \tag{202}$$

$$\exp[D_1\Delta t]\boldsymbol{q}_i = \cos(\zeta_{i1}\Delta t)\boldsymbol{q}_i + \sin(\zeta_{i1}\Delta t)\overleftrightarrow{\boldsymbol{\mathcal{P}}}_1\boldsymbol{q}_i,$$

where

$$\zeta_{i1} = \frac{1}{4I_1s}\boldsymbol{\pi}_i'^T\overleftrightarrow{\boldsymbol{\mathcal{P}}}_1\boldsymbol{q}_i, \tag{203}$$

$$\exp[D_1\Delta t]\boldsymbol{\pi}_i' = \cos(\zeta_{i1}\Delta t)\boldsymbol{\pi}_i' + \sin(\zeta_{i1}\Delta t)\overleftrightarrow{\boldsymbol{\mathcal{P}}}_1\boldsymbol{\pi}_i', \tag{204}$$

$$\exp[D_1\Delta t]P_s = P_s + \left(\sum_{i=1}^{N}\frac{1}{2m_i s^2}\tilde{\boldsymbol{p}}_i^T\overleftrightarrow{\boldsymbol{G}}^{-1}\tilde{\boldsymbol{p}}_i + \sum_{i=1}^{N}2I_1\zeta_{i1}^2 - gk_BT_0\log s + H_0 - gk_BT_0\right)\Delta t, \tag{205}$$

$$\exp[D_1\Delta t]\overleftrightarrow{\boldsymbol{P}}_L = \overleftrightarrow{\boldsymbol{P}}_L + \frac{\Delta t}{V}\left\{\sum_{i=1}^{N}\frac{1}{m_i s}\left[(\overleftrightarrow{\boldsymbol{L}}^T)^{-1}\tilde{\boldsymbol{p}}_i\right]\times\left[(\overleftrightarrow{\boldsymbol{L}}^T)^{-1}\tilde{\boldsymbol{p}}_i\right]^T\right\}\overleftrightarrow{\boldsymbol{\sigma}}, \tag{206}$$

$$\exp[D_2\Delta t]\boldsymbol{q}_i = \cos(\zeta_{i2}\Delta t)\boldsymbol{q}_i + \sin(\zeta_{i2}\Delta t)\overleftrightarrow{\boldsymbol{\mathcal{P}}}_2\boldsymbol{q}_i,$$

where

$$\zeta_{i2} = \frac{1}{4I_2 s}\boldsymbol{\pi}_i'^T\overleftrightarrow{\boldsymbol{\mathcal{P}}}_2\boldsymbol{q}_i, \tag{207}$$

$$\exp[D_2\Delta t]\boldsymbol{\pi}_i' = \cos(\zeta_{i2}\Delta t)\boldsymbol{\pi}_i' + \sin(\zeta_{i2}\Delta t)\overleftrightarrow{\boldsymbol{\mathcal{P}}}_2\boldsymbol{\pi}_i', \tag{208}$$

$$\exp[D_2\Delta t]P_s = P_s + \left(\sum_{i=1}^{N}2I_2\zeta_{i2}^2\right)\Delta t, \tag{209}$$

$$\exp[D_3\Delta t]\boldsymbol{q}_i = \cos(\zeta_{i3}\Delta t)\boldsymbol{q}_i + \sin(\zeta_{i3}\Delta t)\overleftrightarrow{\boldsymbol{\mathcal{P}}}_3\boldsymbol{q}_i,$$

where

$$\zeta_{i3} = \frac{1}{4I_3 s}\boldsymbol{\pi}_i'^T\overleftrightarrow{\boldsymbol{\mathcal{P}}}_3\boldsymbol{q}_i, \tag{210}$$

$$\exp[D_3\Delta t]\boldsymbol{\pi}_i' = \cos(\zeta_{i3}\Delta t)\boldsymbol{\pi}_i' + \sin(\zeta_{i3}\Delta t)\overleftrightarrow{\boldsymbol{\mathcal{P}}}_3\boldsymbol{\pi}_i', \tag{211}$$

$$\exp[D_3\Delta t]P_s = P_s + \left(\sum_{i=1}^{N}2I_3\zeta_{i3}^2\right)\Delta t, \tag{212}$$

$$\exp[D_4\Delta t]P_s = P_s - \frac{\Delta t}{2W}\mathrm{Tr}(\overleftrightarrow{\boldsymbol{P}}_L^T\overleftrightarrow{\boldsymbol{P}}_L), \tag{213}$$

$$\exp[D_4\Delta t]\overleftrightarrow{\boldsymbol{L}} = \overleftrightarrow{\boldsymbol{L}} + \frac{s\Delta t}{W}\overleftrightarrow{\boldsymbol{P}}_L, \tag{214}$$

$$\exp[D_5\Delta t]\tilde{\boldsymbol{p}}_i = \tilde{\boldsymbol{p}}_i + s\overleftrightarrow{\boldsymbol{L}}^T\boldsymbol{F}_i\Delta t, \tag{215}$$

$$\exp[D_5\Delta t]\boldsymbol{\pi}_i' = \boldsymbol{\pi}_i' + 2s\overleftrightarrow{\boldsymbol{S}}(\boldsymbol{q}_i)N_i^{(4)}\Delta t, \tag{216}$$

$$\exp[D_5\Delta t]P_s = P_s - [E(\tilde{\boldsymbol{r}}^{\{N\}},\boldsymbol{q}^{\{N\}},\overleftrightarrow{\boldsymbol{L}}) + P_0V]\Delta t, \tag{217}$$

$$\exp[D_5\Delta t]\overleftrightarrow{\boldsymbol{P}}_L = \overleftrightarrow{\boldsymbol{P}}_L + s\Delta t\left(\frac{1}{V}\sum_{i=1}^{N}\boldsymbol{F}_i\boldsymbol{r}_i^T - P_0\overleftrightarrow{\boldsymbol{1}}\right)\overleftrightarrow{\boldsymbol{\sigma}}, \tag{218}$$

$$\exp[D_6\Delta t]s = s\left(1 + \frac{P_s}{2Q}\Delta t\right)^2, \tag{219}$$

$$\exp[D_6\Delta t]P_s = P_s\Big/\left(1 + \frac{P_s}{2Q}\Delta t\right). \tag{220}$$

Note again that Δt will be replaced in a computer program by $\Delta t/2$ for the time propagation by $D_2, D_3, \ldots, D_6$ in Eqs. (207)–(220). Taking the matrix $\overleftrightarrow{\boldsymbol{L}}$ symmetric ($\overleftrightarrow{\boldsymbol{L}}^T = \overleftrightarrow{\boldsymbol{L}}$), the symplectic integrator for the Nosé-Klein form[20] of the Parrinello-Rahman barostat[19] is also obtained in the same manner.

G. Symplectic condition and time reversibility

In this section we discuss the symplectic condition and the time reversibility.[9] Let us consider a time-independent canonical transformation from

$$\boldsymbol{\Gamma} = \begin{pmatrix}\boldsymbol{Q}\\ \boldsymbol{P}\end{pmatrix} \tag{221}$$

to

$$\boldsymbol{\Gamma}' = \begin{pmatrix}\boldsymbol{Q}'(\boldsymbol{Q},\boldsymbol{P})\\ \boldsymbol{P}'(\boldsymbol{Q},\boldsymbol{P})\end{pmatrix}, \tag{222}$$

where $\boldsymbol{Q}$ and $\boldsymbol{P}$ are the generalized coordinate and the generalized momentum, respectively. The canonical equation of $\boldsymbol{\Gamma}$ is given by

$$\dot{\boldsymbol{\Gamma}} = \boldsymbol{J}\frac{\partial H}{\partial \boldsymbol{\Gamma}}, \tag{223}$$

where

$$\boldsymbol{J} = \begin{pmatrix}\overleftrightarrow{\boldsymbol{0}} & \overleftrightarrow{\boldsymbol{1}}\\ -\overleftrightarrow{\boldsymbol{1}} & \overleftrightarrow{\boldsymbol{0}}\end{pmatrix}. \tag{224}$$

Because $\boldsymbol{\Gamma}'$ is given by the canonical transformation from $\boldsymbol{\Gamma}$, the canonical equation of $\boldsymbol{\Gamma}'$ is also given by

$$\dot{\boldsymbol{\Gamma}}' = \boldsymbol{J}\frac{\partial H}{\partial \boldsymbol{\Gamma}'}. \tag{225}$$

The time derivative of $\boldsymbol{\Gamma}'(\boldsymbol{\Gamma})$ is derived in another way by the chain rule,

$$\dot{\boldsymbol{\Gamma}}' = \frac{\partial \boldsymbol{\Gamma}'}{\partial \boldsymbol{\Gamma}}\dot{\boldsymbol{\Gamma}} = \boldsymbol{M}\dot{\boldsymbol{\Gamma}} = \boldsymbol{M}\boldsymbol{J}\frac{\partial H}{\partial \boldsymbol{\Gamma}} = \boldsymbol{M}\boldsymbol{J}\boldsymbol{M}^T\frac{\partial H}{\partial \boldsymbol{\Gamma}'}, \tag{226}$$

where $\boldsymbol{M}$ is the Jacobian matrix for the canonical transformation from $\boldsymbol{\Gamma}$ to $\boldsymbol{\Gamma}'$ and its (i,j) element is given by

$$M_{ij} = \frac{\partial \Gamma_i'}{\partial \Gamma_j}. \tag{227}$$

Comparing Eqs. (225) and (226), we obtain the symplectic condition,

$$\boldsymbol{M}\boldsymbol{J}\boldsymbol{M}^T = \boldsymbol{J}. \tag{228}$$

In general, the generalized coordinates and momenta obtained by a Hamiltonian dynamics fulfills the symplectic condition in Eq. (228).

Each factor in the decompositions in Eqs. (45) and (106) is a time propagator based on the corresponding Hamiltonian. For example, $\exp[D_1\Delta t]$ in Eqs. (45) is a time propagator by the Hamiltonian of $H_{\text{NP-RB1}}$. Therefore, the time developments by the decompositions in Eqs. (45) and (106) fulfill the symplectic condition. All variables in Eqs. (56)–(86) are canonical variables such as $\boldsymbol{r}_i$, $\boldsymbol{p}_i'$, $\boldsymbol{q}_i$, $\boldsymbol{\pi}_i'$, s, and P_s. Besides, the time propagator here is decomposed so that the MD algorithm will be time reversible; namely, $\exp[-D\Delta t]\exp[D\Delta t]=1$ holds in Eqs. (45) and (106).

Employing the symplectic MD algorithm, there is a conserved quantity which is close to the Hamiltonian.[3] It means that the long-time deviation of the Hamiltonian is suppressed. Therefore, we can perform a MD simulation more stably than by conventional nonsymplectic algorithms.

From the symplectic condition in Eq. (228), the Jacobian determinant is calculated to be 1:

$$\det \boldsymbol{M} = 1. \tag{229}$$

It means that the phase-space volume is conserved during the simulation. Note that the phase-space-volume conservation is a necessary condition of the symplectic condition and not a sufficient condition. The condition that the Jacobian determinant is one does not always mean symplectic. Even if the Jacobian determinant is 1, there is not always conserved quantity which is close to the Hamiltonian. In other words, there are nonsymplectic MD algorithms which are phase-space volume conserving and time reversible. The time propagators in these nonsymplectic algorithms are not based on Hamiltonian and the variables are not canonical variables. That is, the symplectic condition in Eq. (228) is not fulfilled. Therefore, there is no conserved quantity which is close to the Hamiltonian. It means that the value of the Hamiltonian deviates gradually from its initial value in a long-time simulation. In the next section we compare our symplectic algorithm with the nonsymplectic time-reversible algorithms.

III. COMPARISONS WITH NONSYMPLECTIC TIME-REVERSIBLE ALGORITHMS

In this section we explain three nonsymplectic algorithms in the canonical ensemble, which are time reversible. We then apply our symplectic algorithm and these nonsymplectic algorithms to a rigid-body water model and compare them numerically.

A. Molecular dynamics algorithm based on the Nosé-Poincaré thermostat and the nonsymplectic rigid-body algorithm

Instead of the symplectic rigid-body MD algorithm by Miller *et al.*,[5] we here combine the nonsymplectic rigid-body MD algorithm by Matubayasi and Nakahara[4] with the Nosé-Poincaré thermostat.[11,12] In this algorithm, angular velocity $\boldsymbol{\omega}_i' \equiv s\boldsymbol{\omega}_i$ instead of $\boldsymbol{\pi}_i'$ is employed, that is, the variables here are $\boldsymbol{r}_i$, $\boldsymbol{p}_i'$, $\boldsymbol{q}_i$, $\boldsymbol{\omega}_i'$, s, and P_s.

The time propagator $\exp[D\Delta t]$ is decomposed as

$$\begin{aligned}\exp[D\Delta t] = {} & \exp\left[D_5\frac{\Delta t}{2}\right]\exp\left[D_4\frac{\Delta t}{2}\right]\exp\left[D_3\frac{\Delta t}{2}\right] \\ & \times\exp\left[D_2\frac{\Delta t}{2}\right]\exp[D_1\Delta t]\exp\left[D_2\frac{\Delta t}{2}\right] \\ & \times\exp\left[D_3\frac{\Delta t}{2}\right]\exp\left[D_4\frac{\Delta t}{2}\right]\exp\left[D_5\frac{\Delta t}{2}\right] \\ & + O((\Delta t)^3).\end{aligned} \tag{230}$$

where each time propagator is given by

$$\begin{aligned}D_1 = {} & \sum_{i=1}^{N}\frac{\boldsymbol{p}_i'}{m_i s}\cdot\frac{\partial}{\partial \boldsymbol{r}_i} + \sum_{i=1}^{N}\frac{1}{2s}(\overleftrightarrow{\boldsymbol{S}}(\boldsymbol{q}_i)\boldsymbol{\omega}_i'^{(4)})\cdot\frac{\partial}{\partial \boldsymbol{q}_i} \\ & + \left[\sum_{i=1}^{N}\frac{\boldsymbol{p}_i'^2}{2m_i s^2} + \sum_{i=1}^{N}\frac{1}{2s^2}\boldsymbol{\omega}_i'^{(4)T}\overleftrightarrow{\boldsymbol{D}}_i\boldsymbol{\omega}_i'^{(4)} - gk_BT_0\log s \right. \\ & \left. + H_0 + gk_BT_0\right]\frac{\partial}{\partial P_s},\end{aligned} \tag{231}$$

$$D_2 = \sum_{i=1}^{N}\frac{I_{iy}-I_{iz}}{I_{ix}s}\omega_{iy}'\omega_{iz}'\frac{\partial}{\partial\omega_{ix}'} + \sum_{i=1}^{N}\frac{I_{iz}-I_{iy}}{I_{iz}s}\omega_{ix}'\omega_{iy}'\frac{\partial}{\partial\omega_{iz}'}, \tag{232}$$

$$D_3 = \sum_{i=1}^{N}\frac{I_{iz}-I_{ix}}{I_{iy}s}\omega_{iz}'\omega_{ix}'\frac{\partial}{\partial\omega_{iy}'} + \sum_{i=1}^{N}\frac{I_{ix}-I_{iz}}{I_{iz}s}\omega_{ix}'\omega_{iy}'\frac{\partial}{\partial\omega_{iz}'}, \tag{233}$$

$$\begin{aligned}D_4 = {} & \sum_{i=1}^{N}s\boldsymbol{F}_i\cdot\frac{\partial}{\partial\boldsymbol{p}_i'} + \sum_{i=1}^{N}s(\boldsymbol{I}_i^{-1}\boldsymbol{N}_i)\cdot\frac{\partial}{\partial\boldsymbol{\omega}_i'} \\ & - \sum_{i=1}^{N}E(\boldsymbol{r}^{\{N\}},\boldsymbol{q}^{\{N\}})\frac{\partial}{\partial P_s},\end{aligned} \tag{234}$$

$$D_5 = \frac{sP_s}{Q}\frac{\partial}{\partial s} - \frac{P_s^2}{2Q}\frac{\partial}{\partial P_s}. \tag{235}$$

B. Molecular dynamics algorithm based on the Nosé-Hoover thermostat and the symplectic rigid-body algorithm

We here combine the symplectic rigid-body MD algorithm[5] with the Nosé-Hoover thermostat[6–8,10] (the latter is nonsymplectic). This combination has been employed in Ref. 16. Instead of s and P_s, $\eta=\log s$ and $\xi=P_s/Q$ are used for the thermostat, that is, the variables employed here are $\boldsymbol{r}_i$, $\boldsymbol{p}_i$, $\boldsymbol{q}_i$, $\boldsymbol{\pi}_i$, η, and ξ.

The time propagator $\exp[D\Delta t]$ is decomposed as[10]

$$\exp[D\Delta t] = \exp\left[D_6\frac{\Delta t}{4}\right]\exp\left[D_5\frac{\Delta t}{2}\right]\exp\left[D_6\frac{\Delta t}{4}\right]\exp\left[D_4\frac{\Delta t}{2}\right]\exp\left[D_3\frac{\Delta t}{2}\right]$$
$$\times\exp\left[D_2\frac{\Delta t}{2}\right]\exp[D_1\Delta t]\exp\left[D_2\frac{\Delta t}{2}\right]\exp\left[D_3\frac{\Delta t}{2}\right]\exp\left[D_4\frac{\Delta t}{2}\right]\exp\left[D_6\frac{\Delta t}{4}\right]\exp\left[D_5\frac{\Delta t}{2}\right]\exp\left[D_6\frac{\Delta t}{4}\right]$$
$$+ O((\Delta t)^3), \tag{236}$$

where each time propagator is given by[16]

$$D_1 = \sum_{i=1}^{N}\frac{\boldsymbol{p}_i}{m_i}\cdot\frac{\partial}{\partial \boldsymbol{r}_i} + \sum_{i=1}^{N}\frac{1}{4I_1}(\boldsymbol{\pi}_i^T\overleftrightarrow{\mathcal{P}}_1\boldsymbol{q}_i)(\overleftrightarrow{\mathcal{P}}_1\boldsymbol{q}_i)\cdot\frac{\partial}{\partial \boldsymbol{q}_i}$$
$$+ \sum_{i=1}^{N}\frac{1}{4I_1}(\boldsymbol{\pi}_i^T\overleftrightarrow{\mathcal{P}}_1\boldsymbol{q}_i)(\overleftrightarrow{\mathcal{P}}_1\boldsymbol{\pi}_i)\cdot\frac{\partial}{\partial \boldsymbol{\pi}_i}, \tag{237}$$

$$D_2 = \sum_{i=1}^{N}\frac{1}{4I_2}(\boldsymbol{\pi}_i^T\overleftrightarrow{\mathcal{P}}_2\boldsymbol{q}_i)(\overleftrightarrow{\mathcal{P}}_2\boldsymbol{q}_i)\cdot\frac{\partial}{\partial \boldsymbol{q}_i} + \sum_{i=1}^{N}\frac{1}{4I_2}(\boldsymbol{\pi}_i^T\overleftrightarrow{\mathcal{P}}_2\boldsymbol{q}_i)$$
$$\times(\overleftrightarrow{\mathcal{P}}_2\boldsymbol{\pi}_i)\cdot\frac{\partial}{\partial \boldsymbol{\pi}_i}, \tag{238}$$

$$D_3 = \sum_{i=1}^{N}\frac{1}{4I_3}(\boldsymbol{\pi}_i^T\overleftrightarrow{\mathcal{P}}_3\boldsymbol{q}_i)(\overleftrightarrow{\mathcal{P}}_3\boldsymbol{q}_i)\cdot\frac{\partial}{\partial \boldsymbol{q}_i} + \sum_{i=1}^{N}\frac{1}{4I_3}(\boldsymbol{\pi}_i^T\overleftrightarrow{\mathcal{P}}_3\boldsymbol{q}_i)$$
$$\times(\overleftrightarrow{\mathcal{P}}_3\boldsymbol{\pi}_i)\cdot\frac{\partial}{\partial \boldsymbol{\pi}_i}, \tag{239}$$

$$D_4 = \sum_{i=1}^{N}\boldsymbol{F}_i\cdot\frac{\partial}{\partial \boldsymbol{p}_i} + \sum_{i=1}^{N}2(\overleftrightarrow{\boldsymbol{S}}(\boldsymbol{q}_i)\boldsymbol{N}_i^{(4)})\cdot\frac{\partial}{\partial \boldsymbol{\pi}_i}, \tag{240}$$

$$D_5 = -\xi\sum_{i=1}^{N}\boldsymbol{p}_i\cdot\frac{\partial}{\partial \boldsymbol{p}_i} - \xi\sum_{i=1}^{N}\boldsymbol{\pi}_i\cdot\frac{\partial}{\partial \boldsymbol{\pi}_i} + \xi\frac{\partial}{\partial \eta}, \tag{241}$$

$$D_6 = \frac{1}{Q}\left(\sum_{i=1}^{N}\frac{\boldsymbol{p}_i^2}{m_i} + \sum_{i=1}^{N}\frac{1}{4}\boldsymbol{\pi}_i^T\overleftrightarrow{\boldsymbol{S}}(\boldsymbol{q}_i)\overleftrightarrow{\boldsymbol{D}}_i\overleftrightarrow{\boldsymbol{S}}^T(\boldsymbol{q}_i)\boldsymbol{\pi}_i - gk_BT_0\right)\frac{\partial}{\partial \xi}. \tag{242}$$

We remark that we can also make another second-order integrator by the decomposition in Eq. (106) instead of Eq. (236). However, the original time reversible algorithm for the Nosé-Hoover thermostat decomposed the time propagator as in Eq. (236),[10] thus we used this decomposition.

C. Molecular dynamics algorithm based on the Nosé-Hoover thermostat and the symplectic rigid-body algorithm

We can also make a nonsymplectic algorithm by the rigid-body algorithm by Matubayasi and Nakahara[4] and the Nosé-Hoover thermostat.[6–8,10] In this algorithm the following variables are developed with time: $\boldsymbol{r}_i$, $\boldsymbol{p}_i$, $\boldsymbol{q}_i$, $\boldsymbol{\omega}_i$, η, and ξ.

The time propagator $\exp[D\Delta t]$ is decomposed as in Eq. (236). Each decomposed time propagator is given by

$$D_1 = \sum_{i=1}^{N}\frac{\boldsymbol{p}_i}{m_i}\cdot\frac{\partial}{\partial \boldsymbol{r}_i} + \sum_{i=1}^{N}\frac{1}{2}(\overleftrightarrow{\boldsymbol{S}}(\boldsymbol{q}_i)\boldsymbol{\omega}_i^{(4)})\cdot\frac{\partial}{\partial \boldsymbol{q}_i}, \tag{243}$$

$$D_2 = \sum_{i=1}^{N}\frac{I_{iy}-I_{iz}}{I_{ix}}\omega_{iy}\omega_{iz}\frac{\partial}{\partial \omega_{ix}} + \sum_{i=1}^{N}\frac{I_{iz}-I_{iy}}{I_{iz}}\omega_{ix}\omega_{iy}\frac{\partial}{\partial \omega_{iz}}, \tag{244}$$

$$D_3 = \sum_{i=1}^{N}\frac{I_{iz}-I_{ix}}{I_{iy}}\omega_{iz}\omega_{ix}\frac{\partial}{\partial \omega_{iy}} + \sum_{i=1}^{N}\frac{I_{ix}-I_{iz}}{I_{iz}}\omega_{ix}\omega_{iy}\frac{\partial}{\partial \omega_{iz}}, \tag{245}$$

$$D_4 = \sum_{i=1}^{N}\boldsymbol{F}_i\cdot\frac{\partial}{\partial \boldsymbol{p}_i} + \sum_{i=1}^{N}(\boldsymbol{I}_i^{-1}\boldsymbol{N}_i)\cdot\frac{\partial}{\partial \boldsymbol{\omega}_i}, \tag{246}$$

$$D_5 = -\xi\sum_{i=1}^{N}\boldsymbol{p}_i\cdot\frac{\partial}{\partial \boldsymbol{p}_i} - \xi\sum_{i=1}^{N}\boldsymbol{\omega}_i\cdot\frac{\partial}{\partial \boldsymbol{\omega}_i} + \xi\frac{\partial}{\partial \eta}, \tag{247}$$

$$D_6 = \frac{1}{Q}\left(\sum_{i=1}^{N}\frac{\boldsymbol{p}_i^2}{m_i} + \sum_{i=1}^{N}\boldsymbol{\omega}_i^{(4)T}\overleftrightarrow{\boldsymbol{D}}_i\boldsymbol{\omega}_i^{(4)} - gk_BT_0\right)\frac{\partial}{\partial \xi}. \tag{248}$$

D. Numerical comparisons: Application to a pure water system

We applied the symplectic and nonsymplectic MD algorithms to a rigid-body model of water in the canonical ensemble. We employed the TIP3P rigid-body model for the water molecules.[21] We used 80 water molecules in a cubic unit cell with periodic boundary conditions. The temperature was set at 300 K and the mass density was set to 0.997 g/cm^3. The electrostatic potential was calculated by the Ewald method. We calculated the van der Waals interaction, which is given by the Lennerd-Jones term, of all pairs of the molecules within the minimum image convention instead of introducing the spherical potential cutoff. If one introduces a potential cutoff carelessly, the potential energy will not be a continuous function and the Hamiltonian will not be conserved. In order to check the Hamiltonian conservation, we avoided such an artifact induced by the potential energy cutoff. We tested the time steps of Δt=2, 3, 4, and 5 fs. We performed the MD simulations for 1.5 ns in all cases of Δt. We employed Eqs. (56)–(86) for the Nosé-Poincaré thermostat and symplectic rigid-body MD simulations, Eqs. (231)–(235) for the Nosé-Poincaré thermostat and nonsymplectic rigid-body MD simulations, Eqs. (237)–(242)

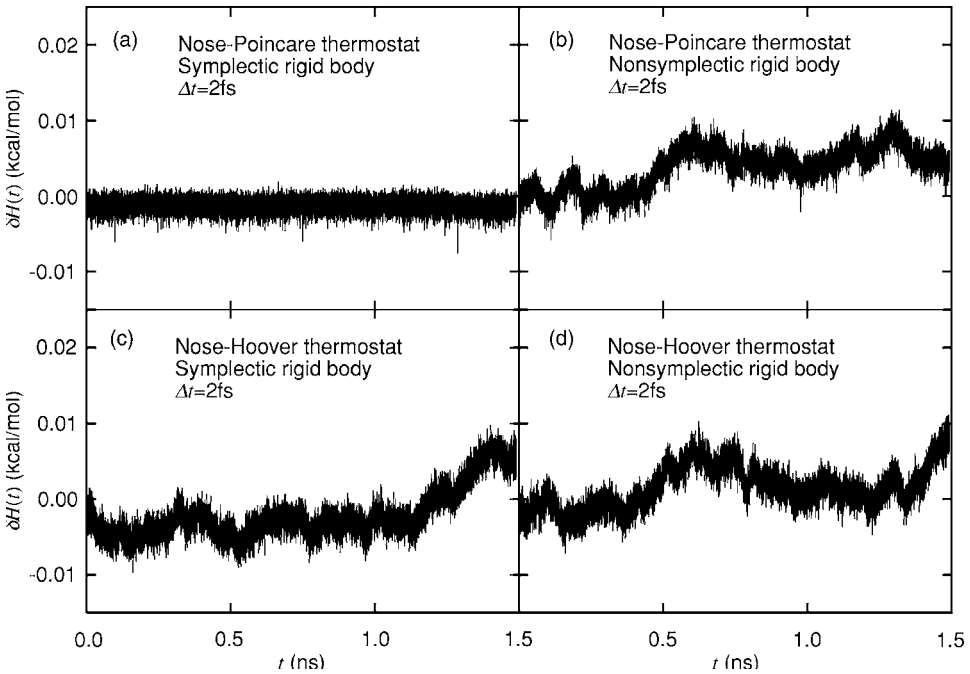

FIG. 1. The time series of the difference $\delta H(t)$ of Hamiltonian from its initial value. The time step was set to $\Delta t=2$ fs. (a) Nosé-Poincaré thermostat and symplectic rigid-body MD, (b) Nosé-Poincaré thermostat and nonsymplectic rigid-body MD, (c) Nosé-Hoover thermostat and symplectic rigid-body MD, and (d) Nosé-Hoover thermostat and nonsymplectic rigid-body MD.

for the Nosé-Hoover thermostat and symplectic rigid-body MD simulations, and the time development in Eqs. (243)–(248) for the Nosé-Hoover thermostat and nonsymplectic rigid-body MD simulations. The same initial conditions were used for all algorithms and time steps.

We observed the deviations of the Nosé Hamiltonian from its initial values,

$$\delta H(t) = \sum_{i=1}^{N} \frac{\boldsymbol{p}_i'^2}{2m_i s^2} + \sum_{i=1}^{N} \frac{1}{8s^2} \boldsymbol{\pi}_i'^T \overleftrightarrow{\boldsymbol{S}}(\boldsymbol{q}_i) \overleftrightarrow{\boldsymbol{D}}_i \overleftrightarrow{\boldsymbol{S}}^T(\boldsymbol{q}_i) \boldsymbol{\pi}_i' + E(\boldsymbol{r}^{\{N\}}, \boldsymbol{q}^{\{N\}}) + \frac{P_s^2}{2Q} + g k_B T_0 \log s - H_0. \quad (249)$$

Figures 1–4 show $\delta H(t)$ for $\Delta t=2$, 3, 4, and 5 fs, respectively. The gradient of the linear fitting for each $\delta H(t)$ is shown in Table I.

In every nonsymplectic MD algorithm, the Hamiltonian deviates from its initial value as time passes even for $\Delta t=2$ fs as shown in Figs. 1(b)–1(d). This deviation increases as the time step increases from $\Delta t=2$ to 5 fs as shown in Figs. 2–4. Note that the energy scale in the ordinate increases as Δt increases.

On the other hand, the Nosé-Poincaré thermostat and symplectic rigid-body MD algorithm guarantees the existence of a conserved quantity which is close to the Hamiltonian. Because of this conserved quantity, the difference $\delta H(t)$ was suppressed well for time steps of $\Delta t=2$, 3, and 4 fs as shown in Figs. 1(a)–3(a). The Hamiltonian starts to

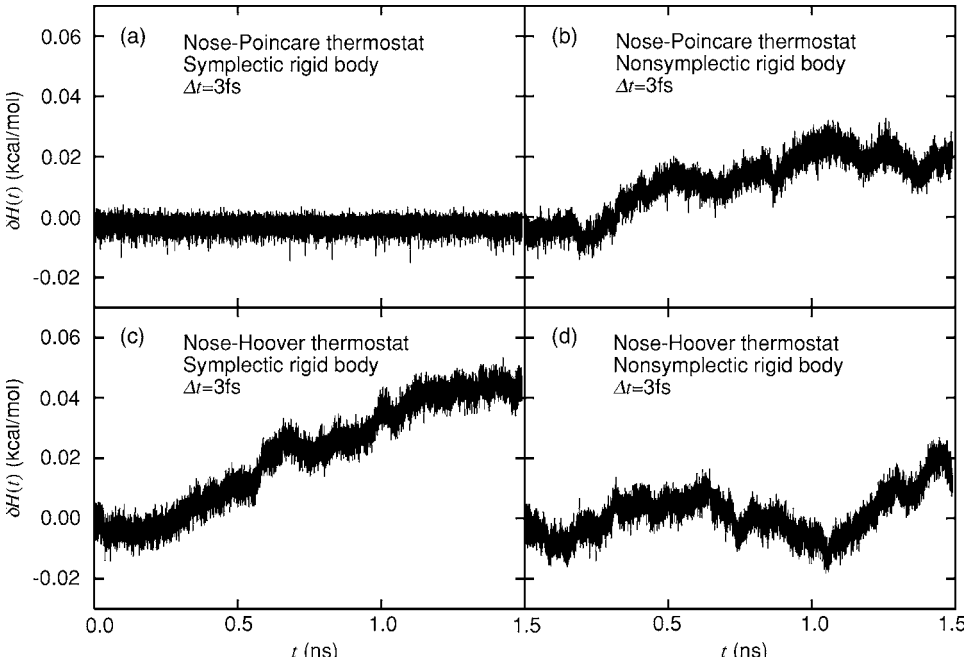

FIG. 2. The time series of $\delta H(t)$. The time step was set to $\Delta t=3$ fs (see the caption of Fig. 1 for further details).

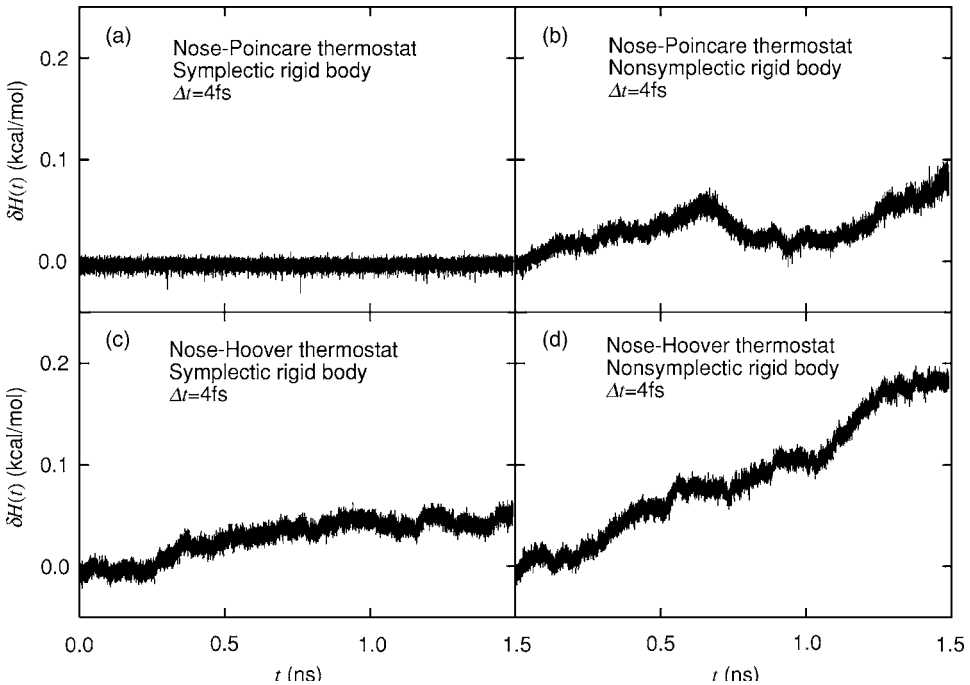

FIG. 3. The time series of $\delta H(t)$. The time step was set to $\Delta t=4$ fs (see the caption of Fig. 1 for further details).

deviate slightly by $d\delta H(t)/dt=3.7\times10^{-3}$ kcal/mol ns in the case of $\Delta t=5$ fs as shown in Table I and Fig. 4(a). However, the other nonsymplectic integrators perform much worse here. They deviate by the order of $d\delta H(t)/dt=10^{-1}$ kcal/mol ns (see Table I). This fact implies that by employing the combination of the Nosé-Poincaré thermostat and the symplectic rigid-body algorithm, one can take a time step of as much as 4 fs. This time step is longer than typical values of 0.5–2 fs which are used by the conventional nonsymplectic algorithms.

We comment here on the temperature control by the Nosé-Poincaré thermostat. Figure 5 shows the difference of temperature calculated by the MD simulations from its preset value of $T_0=300$ K:

$$\langle T\rangle - T_0 = \left\langle \frac{1}{6Nk_B}\left(\sum_{i=1}^{N}\frac{\boldsymbol{p}_i^2}{m_i}+\sum_{i=1}^{N}\boldsymbol{\omega}_i^T\vec{\boldsymbol{I}}_i\boldsymbol{\omega}_i\right)\right\rangle - T_0. \quad (250)$$

The error bars were estimated by the jackknife method[22] by dividing the production run into ten segments. In the case that the Nosé-Poincaré thermostat was employed, this deviation is larger than that by the Nosé-Hoover thermostat. Figure 5(a) shows that this deviation by the symplectic rigid-body integrator with the Nosé-Poincaré thermostat is of the order of $(\Delta t)^2$ as for $\Delta t=2$, 3, and 4 fs. The straight line in Fig. 5(a) was determined by the least-squares fitting for the data at $\Delta t=2$, 3, and 4 fs to

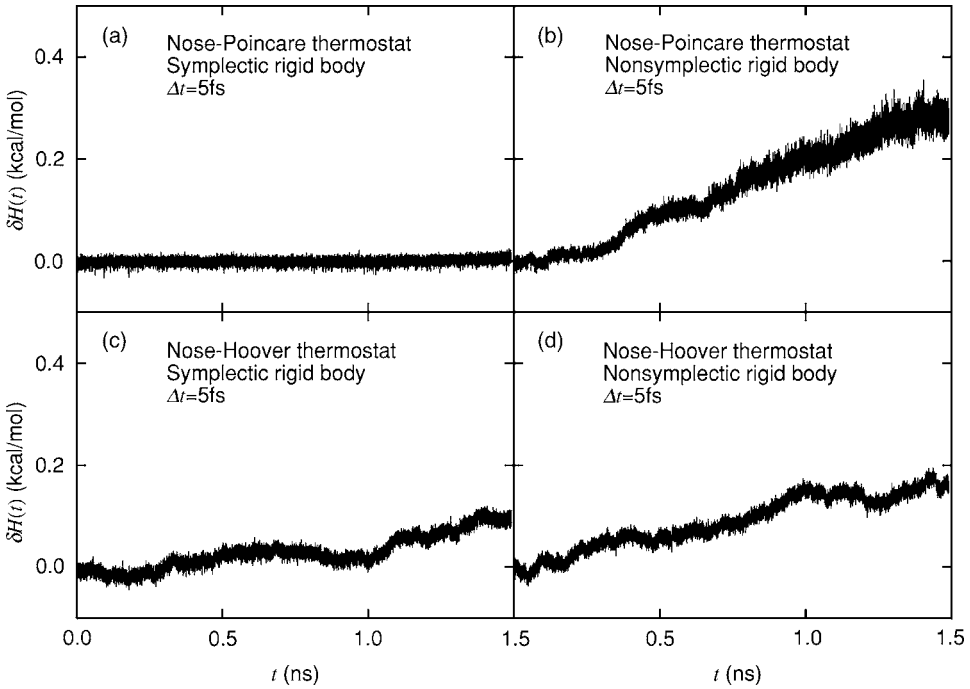

FIG. 4. The time series of $\delta H(t)$. The time step was set to $\Delta t=5$ fs (see the caption of Fig. 1 for further details).

TABLE I. Drift of the Hamiltonian per nanosecond $d\delta H/dt$ (kcal/mol ns).

Δt	2 fs	3 fs	4 fs	5 fs
Nosé-Poincaré and symplectic rigid-body MD	-1.4×10^{-4}	-3.0×10^{-4}	2.0×10^{-4}	3.7×10^{-3}
Nosé-Poincaré and nonsymplectic rigid-body MD	4.4×10^{-3}	1.9×10^{-2}	2.8×10^{-2}	2.2×10^{-1}
Nosé-Hoover and symplectic rigid-body MD	5.3×10^{-3}	3.9×10^{-2}	3.8×10^{-2}	6.9×10^{-2}
Nosé-Hoover and nonsymplectic rigid-body MD	2.9×10^{-3}	7.3×10^{-3}	1.3×10^{-1}	1.2×10^{-1}

$$\langle T\rangle - T_0 = a(\Delta t)^2, \tag{251}$$

where a is a fitting parameter. This deviation possibly comes from the equations of motion for the Nosé-Poincaré thermostat. It is not due to the combination of the Nosé-Poincaré thermostat and the symplectic rigid-body MD algorithm. The conserved quantity $\tilde{H}$ in the Nosé-Poincaré thermostat has a difference of the order of $(\Delta t)^2$ from the original Nosé-Poincaré Hamiltonian $H_{\mathrm{NP}}=s[H_{\mathrm{N}}-H_0]$,

$$\tilde{H} = s[H_N(\boldsymbol{r}^{\{N\}},\boldsymbol{p}'^{\{N\}},s,P_s) - H_0] + O((\Delta t)^2). \tag{252}$$

The dynamics of the actual symplectic MD simulation is based on $\tilde{H}$ rather than H_{N}. The conserved quantity $\tilde{H}$ has a role of the Hamiltonian for the dynamics of the symplectic MD simulation and is here referred to as the virtual Hamiltonian. Based on $\tilde{H}$, Eq. (6) is rewritten as

$$\dot{P}_s = \sum_{i=1}^{N} \frac{\boldsymbol{p}_i^2}{m_i} - gk_BT_0 - [H_{\mathrm{N}}(\boldsymbol{r}^{\{N\}},\boldsymbol{p}'^{\{N\}},s,P_s) - H_0] + O((\Delta t)^2). \tag{253}$$

The error term of the order of $(\Delta t)^2$ comes from the virtual Hamiltonian $\tilde{H}$ in Eq. (252). This difference means that T_0 is practically modified in the order of $(\Delta t)^2$ in Eq. (253). This is why the average temperature $\langle T\rangle$ was different from T_0 by the order of $(\Delta t)^2$. One possible method to alleviate this temperature deviation is to reset the value of H_0 so that it will compensate for the term of $O((\Delta t)^2)$ in Eq. (253). Although the Hamiltonian conservation is excellent by the symplectic rigid-body MD integrator with the Nosé-Poincaré thermostat, one has to pay attention to the temperature control. In the case of $\Delta t=5$ fs, the deviation $\langle T\rangle-T_0$ is not on the line in Eq. (251). This is because H_{N} gradually increases as time passes [see Fig. 4(a)]. In the combined algorithm of the Nosé-Poincaré thermostat and nonsymplectic rigid-body MD algorithm, H_{N} increases as time passes as well [see Figs. 1(b)–4(b)]. The deviation $\langle T\rangle-T_0$ is thus not on the line in Eq. (251) as shown in Fig. 5(b). In the case of the Nosé-Hoover thermostat [see Figs. 5(c) and 5(d)], $\langle T\rangle$ also deviates from T_0 as Δt increases, although its deviation is much smaller than that by the Nosé-Poincaré thermostat.

IV. CONCLUSIONS

We have proposed an explicit symplectic MD algorithm for rigid-body molecules in the canonical ensemble. This algorithm is based on the Nosé-Poincaré thermostat[11,12] and the symplectic rigid-body algorithm.[5] We have also presented an explicit symplectic MD algorithm for rigid-body molecules in the isobaric-isothermal ensembles by combining the Andersen barostat[17] with the symplectic algorithm in the canonical ensemble. As a modification of the isobaric-isothermal algorithm, we further presented the symplectic integrator in the constant normal pressure and lateral surface area ensemble and a symplectic algorithm combined with the

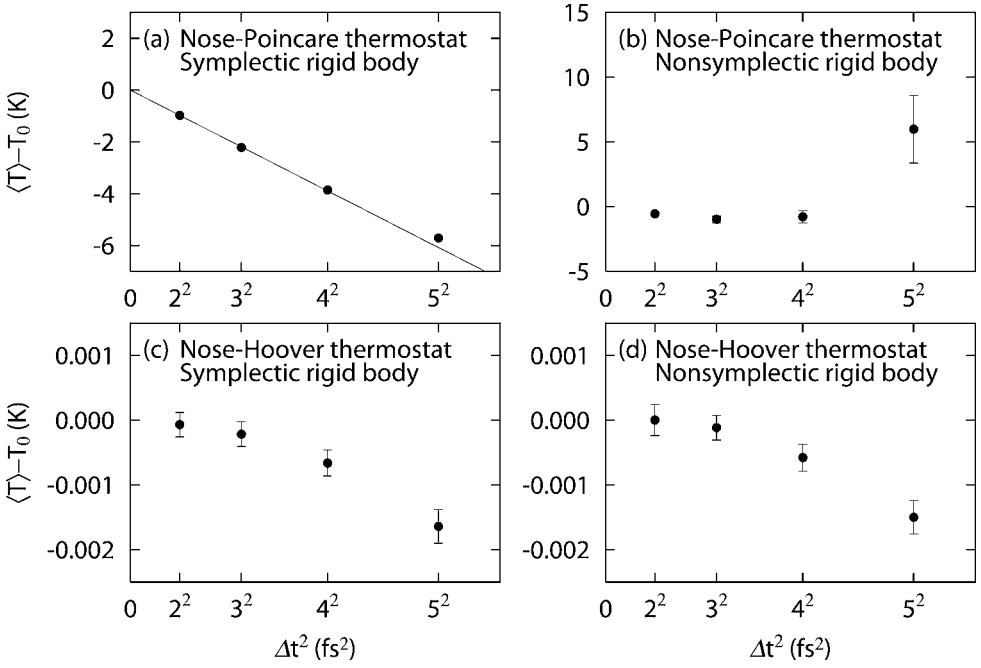

FIG. 5. The deviations of temperature $\langle T\rangle-T_0$ as functions of the square of the time step $(\Delta t)^2$ (see the caption of Fig. 1 for further details).

Parrinello-Rahman algorithm. Employing the symplectic MD algorithm, there is a conserved quantity which is close to the Hamiltonian. Therefore, we can perform a MD simulation more stably than by conventional nonsymplectic algorithms.

In order to establish this fact numerically, we have applied this algorithm to a TIP3P pure water system at 300 K and compared the time evolution of the Hamiltonian with those by the nonsymplectic algorithms. These nonsymplectic algorithms are based on the Nosé-Poincaré thermostat[11,12] and the nonsymplectic rigid-body algorithm,[4] based on the Nosé-Hoover thermostat[10] and the symplectic rigid-body algorithm,[5] and based on the Nosé-Hoover thermostat[10] and the nonsymplectic rigid-body algorithm.[4] In these nonsymplectic algorithms, the Hamiltonian deviates gradually from its initial value in all cases of the time steps $\Delta t=2$, 3, 4, and 5 fs. On the other hand, the Hamiltonian was conserved well even for a time step of 4 fs in our symplectic algorithm.

The rigid-body model for molecules can be employed not only for a water system but also for a biomolecular system. For example, a partial rigid-body model[16] is often used for a part of a peptide and a protein, in particular, for a hydrogen-including part such as a methyl group ($-CH_3$) to alleviate a fast motion of the hydrogen atom. In the case of the methyl group, the C–H bond length and the H–C–H bond angles are fixed as a rigid-body model. On the other hand, the dihedral angles including the C–H bond (X–X–C–H, where X stands for an arbitrary atom) varies depending on the methyl group motion and is calculated in the same way as in the flexible model. Our algorithms will thus be of great use for MD simulations of an aqueous solution and a biomolecular system at a constant temperature and/or pressure.

ACKNOWLEDGMENTS

This work was supported, in part, by the Grants-in-Aid for the Next Generation Super Computing Project, Nanoscience Program, and for Scientific Research in Priority Areas, "Water and Biomolecules," from the Ministry of Education, Culture, Sports, Science and Technology, Japan.

[1] J. P. Ryckaert, G. Ciccotti, and H. J. C. Berendsen, J. Comput. Phys. **23**, 327 (1977).
[2] C. W. Gear, *Numerical Initial Value Problems in Ordinary Differential Equations* (Prentice-Hall, Englewood Cliffs, NJ, 1971), Ch. 9, p. 136.
[3] H. Yoshida, Phys. Lett. A **150**, 262 (1990).
[4] N. Matubayasi and M. Nakahara, J. Chem. Phys. **110**, 3291 (1999).
[5] T. F. MillerIII, M. Eleftheriou, P. Pattnaik, A. Ndirango, D. Newns, and G. J. Martyna, J. Chem. Phys. **116**, 8649 (2002).
[6] S. Nosé, Mol. Phys. **52**, 255 (1984).
[7] S. Nosé, J. Chem. Phys. **81**, 511 (1984).
[8] W. G. Hoover, Phys. Rev. A **31**, 1695 (1985).
[9] H. Goldstein, C. Poole, and J. Safko, *Classical Mechanics*, 3rd ed. (Addison-Wesley, San Francisco, 2002), Ch. 9, p. 368.
[10] G. J. Martyna, M. E. Tuckerman, D. J. Tobias, and M. L. Klein, Mol. Phys. **87**, 1117 (1996).
[11] S. D. Bond, B. J. Leimkuhler, and B. B. Laird, J. Comput. Phys. **151**, 114 (1999).
[12] S. Nosé, J. Phys. Soc. Jpn. **70**, 75 (2001).
[13] H. Okumura and Y. Okamoto, Chem. Phys. Lett. **391**, 248 (2004).
[14] H. Okumura and Y. Okamoto, J. Comput. Chem. **27**, 379 (2006).
[15] H. Okumura and Y. Okamoto, Bull. Chem. Soc. Jpn. 80 (2007) (in press).
[16] M. Ikeguchi, J. Comput. Chem. **25**, 529 (2004).
[17] H. C. Andersen, J. Chem. Phys. **72**, 2384 (1980).
[18] H. Goldstein, C. Poole, and J. Safko, *Classical Mechanics*, 3rd ed. (Addison-Wesley, San Francisco, 2002), Ch. 5, p. 184.
[19] M. Parrinello and A. Rahman, Phys. Rev. Lett. **45**, 1199 (1980).
[20] S. Nosé and M. L. Klein, Mol. Phys. **50**, 1055 (1983).
[21] W. L. Jorgensen, J. Chandrasekhar, J. D. Madura, R. W. Impey, and M. L. Klein, J. Chem. Phys. **79**, 926 (1983).
[22] B. A. Berg, *Introduction to Monte Carlo Simulations and Their Statistical Analysis* (World Scientific, Singapore, 2004).